Ingineria automobilului

Automotive engineering

Registrul Auto Român

SIAR

Societatea Inginerilor de Automobile din România

OFICIAL JOURNAL OF THE SOCIETY OF AUTOMOTIVE ENGINEERS OF ROMANIA – SIAR ISSN 1842 – 4074
SPONSORED BY THE ROMANIAN AUTOMOTIVE REGISTER – RAR OPEN ACCESS NR. 80/SEPTEMBRIE 2026

UNIvIA 2026 – Ediția a VIII-a 22.07 – 24.07.2026, SIAR, RAR, ATM F1



• Despre influența inscripțiilor magnetice aplicate pe vehicule asupra siguranței rutiere și funcționării senzorilor auto • Sistem de cogenerare cu motor diesel D110 pentru mobilitate electrică și încălzire rezidențială • Optimizarea eficienței energetice a sistemului de propulsie al vehiculelor autonome • Analiza numerică a unei geometrii a pistonului destinată intensificării turbulenței într-un motor cu ardere internă cu aprindere prin comprimare

SIAR ESTE MEMBRĂ FISITA INTERNATIONAL FEDERATION OF AUTOMOTIVE ENGINEERING SOCIETIES

EAEC EUROPEAN AUTOMOBILE ENGINEERS COOPERATION

APARE TRIMESTRIAL
QUARTERLY
FREE OF CHARGE

The 36th International Congress of Automotive and Transport Engineering

MOBILITY ENGINEERING AND SUSTAINABILITY

5 -7 November 2026, Pitești, Romania

ENDORSED BY FISITA

Congress Themes:

1. *Accident Research and Analysis*
2. *Active and Passive Safety*
3. *Advanced Engineering Methods (CAx)*
4. *Advanced Materials, Manufacturing Technologies and Logistics*
5. *Advanced Transport Systems and Road Traffic*
6. *Heavy and Special Vehicles*
7. *Hybrid & Electric Vehicles*
8. *Internal Combustion Engines*
9. *Transmission Systems*
10. *Vehicle Electronics and Software*

The CAR Conference/Congress is a traditional scientific event initiated by University of Pitesti in **1978**. Starting with its 5th edition organized in 1992, CAR International Conference became one of the SIAR Conferences. **CAR Congress reaching its 12th edition this year**, is part of the SIAR's series of similar annual scientific events held successively by various universities in Romania with interests in Automotive Engineering (Transilvania University of Brasov – CONAT Congress, National University of Science and Technology "Politehnica", Bucharest University Center – ESFA Congress, National University of Science and Technology "Politehnica", Pitesti University Center – CAR Congress, Technical University of Cluj-Napoca – AMMA Congress, University of Craiova – SMAT Congress, Polytechnic University of Timisoara – MVT Congress, Moldova Technical University of Chisinau - AITS Congress).
Thus, **CAR2026 is actually the 36th edition of SIAR International Congress.**
The 2026 edition of CAR International Congress is focused on ***MOBILITY ENGINEERING AND SUSTAINABILITY.***
As other SIAR scientific events, **CAR2026** will be an opportunity for delegates to:
- update skills and knowledge by attending focused technical sessions
- gain insights into the automotive industry
- network with potential new partners, clients and suppliers
- view the latest technology products and services in the commercial exhibition

Therefore, academics, researchers, engineers and other specialists in automotive engineering and road transport, students and anyone who is interested are invited to be part of this scientific event. Let us all contribute to its success!

With the support of

SOCIETATEA INGINERILOR DE AUTOMOBILE DIN ROMÂNIA
SOCIETY OF AUTOMOTIVE ENGINEERS OF ROMANIA

Pitești University Center -
National University of Science and Technology POLITEHNICA Bucharest

www.siar.ro
siar@siar.ro

Email: car2026@upit.ro
Website: www.siarcongress.eu
Facebook: https://web.facebook.com/SIAR.CAR/



AN IDEA ABOUT AI IN AUTOMOTIVE ENGINEERING EDUCATION
O IDEE DESPRE AI ÎN FORMAREA INGINERILOR DE AUTOMOBILE



„AI este capacitatea unei mașini de a imita funcții umane, cum ar fi raționamentul, învățarea, planificarea și creativitatea.” [1] În ultimul său eseu publicat pe Gates Notes [2] Bill Gates consideră inteligența artificială drept „una dintre cele mai turbulente și potențial periculoase forțe din istoria omenirii, avertizând că lumea nu este pregătită pentru rapidele schimbări societale pe care le va provoca.” [3] Printre preocupările majore ale lui Bill Gates se înscrie și: „ ... **utilizarea excesivă a AI în educație,** menționând studii timpurii care asociază utilizarea intensă a AI cu scăderea gândirii critice la tineri.” [3]

O primă discuție avută cu puțină vreme în urmă cu colegii din Academia Tehnică Militară „Ferdinand I” din București și apoi o alta (la câteva zile distanță) la Politehnica București m-au determinat să observ că AI este deja prezentă în procesul de formare a inginerilor de automobile din universitățile noastre. Ca mai întotdeauna când avem în vedere exploatarea noilor tehnologii cei care – se pare – au aderat/explorat/testat/utilizat primii cel puțin elemente identificate drept AI au fost studenții noștri! Apreciez și cred că apreciem cu toții acest aspect! Cu condiția ca prin astfel de tehnici să nu se obțină „foloase necuvenite”! Dar, un principiu de drept spune că „nu poate fi pedepsit ceea ce nu este interzis”. Media prezintă frecvent opinii ale unor „experți” (câteodată doar „specialiști”) din care am putea înțelege că într-un viitor nu foarte îndepărtat ne paște fie o „eră de aur în care mașinile/roboții vor munci, iar oamenii vor trândăvi”, fie „apocalipsa”! Se pare că tot Bill Gates ar fi afirmat că majoritatea celor care dezvolta AI nu ar înțelege deplin ce este AI!?

Dar, pot observa lipsa unei dezbateri serioase pe această temă în cadrul comunității noastre academice în condițiile existenței unui proces semnificativ de schimbare a societății noastre!

Cunoaștem că într-o oarecare măsură există filtre ce încearcă să descurajeze practicile neconforme cu etica și spiritul de onestitate promovate continuu în mediul academic. Cu toate acestea, se știe de asemenea, că tentative/acțiuni de ocolire/acoperire/corupere a codurilor de conduită au existat și vor exista. Și atunci se poate pune întrebarea: Ce este de făcut? Preocupați de problemele curente nu observăm efectele deja prezente, neglijăm, considerăm că nu este treaba noastră sau că oricum nu avem ce să facem în legătură cu tema AI întrucât complexitatea problemei ne depășește?

Departe de a propune un model, împărtășesc câteva gânduri legate de măsura în care AI este/ar putea fi implicată/folosită în elaborarea proiectelor de curs, respectiv proiectelor de diplomă. Am putea observa că privitor la acest tip de activitate, ca rezultat al învățării, „studentul/absolventul elaborează proiecte profesionale prin selectarea, combinarea și utilizarea de concepte, principii, metodologii și tehnologii din domeniu”[4]. Simplificând această activitate, identificăm existența unor etape de transmitere către studenți a unei teme de proiect împreună cu detalierea cerințelor, de îndrumare și, în final, de evaluare a proiectului. Și se pune apăsat întrebarea: Ce se evaluează și cum se acordă o notă studentului/absolventului pentru proiectul prezentat în condițiile în care majoritatea activității sale este în afara cadrului reglementat/coordonat - altfel spus „acasă”? Iar la prezentarea/susținerea proiectului (totdeauna în timp limitat) și acordarea unei note se au în vedere rezultatele obținute – altfel spus în ce măsură „produsul” proiectat corespunde cerințelor formulate în tema de proiect primită? Așadar, se acordă notă „produsului” proiectat! Evident, cadrul didactic are o viziune proprie și există o anumită dispersie a parametrilor în cadrul baremelor de notare. Dar, totuși, determinantă în evaluare este măsura în care algoritmii de calcul sunt respectați și rezultatele finale corespund cerințelor.

Și aici ar fi loc pentru câteva comentarii!

La cursul de motoare cu ardere internă studenții vor primi ca tema de proiect proiectarea unui motor! La cursul de organe de mașini vor primi ca temă de proiect proiectarea unui reductor! Și așa mai departe! Teme ce impun studentului/absolventului activități/responsabilități destul de îndepărtate de realitatea în care ar putea lucra ulterior absolvirii!

Continuarea la pagina 26

SUMAR „INGINERIA AUTOMOBILULUI“ NR. 80

3 AN IDEA ABOUT AI IN AUTOMOTIVE ENGINEERING EDUCATION
O IDEE DESPRE AI ÎN FORMAREA INGINERILOR DE AUTOMOBILE

5 THE INFLUENCE OF MAGNETIC INSCRIPTIONS APPLIED TO VEHICLES ON ROAD SAFETY AND THE FUNCTIONING OF CAR SENSORS
INFLUENȚA INSCRIPȚIILOR MAGNETICE APLICATE PE VEHICULE ASUPRA SIGURANȚEI RUTIERE ȘI FUNCȚIONĂRII SENZORILOR AUTO

10 D110 DIESEL ENGINE–BASED COGENERATION SYSTEM FOR ELECTRIC MOBILITY AND RESIDENTIAL HEATING
SISTEM DE COGENERARE CU MOTOR DIESEL D110 PENTRU MOBILITATE ELECTRICĂ ȘI ÎNCĂLZIRE REZIDENȚIALĂ

14 ENERGY EFFICIENCY OPTIMISATION IN AUTONOMOUS VEHICLE POWERTRAIN
OPTIMIZAREA EFICIENȚEI ENERGETICE A SISTEMULUI DE PROPULSIE AL VEHICULELOR AUTONOME

20 NUMERICAL ANALYSIS OF TURBULENCE ENHANCING PISTON GEOMETRY IN A COMPRESSION IGNITION INTERNAL COMBUSTION ENGINE
ANALIZA NUMERICĂ A UNEI GEOMETRII A PISTONULUI DESTINATĂ INTENSIFICĂRII TURBULENȚEI ÎNTR-UN MOTOR CU ARDERE INTERNĂ CU APRINDERE PRIN COMPRIMARE

25 THE EIGHTH EDITION OF THE SIAR SUMMER UNIVERSITY IN AUTOMOTIVE ENGINEERING
A OPTA EDIȚIE A UNIVERSITĂȚII DE VARĂ SIAR ÎN INGINERIA AUTOVEHICULELOR UNIVIA 2026

Foto coperta 1: Daniela VOICU

REGISTRUL AUTO ROMÂN

Director general
Mihai ALECU
Director tehnic
Ing. Cristian Viorel BUCUR

Şef Departament Comunicare şi Redacţie Site Auto Test
Roxana DIMA

Redactori
Sorin BARBU
Emilia PETRE

Contact:
Calea Griviţei 391 A,
sector 1, cod poştal 010719,
Bucureşti, România
Tel/Fax: 021/202.70.00
E-mail: autotest@rarom.ro
www.rarom.ro
www.autotestmagazin.ro

SIAR

Contact
Facultatea de Transporturi
UNST Politehnica Bucureşti
Splaiul Independenţei 313
Sala JC005 Cod poştal 060042
Sector 6 Bucureşti România
Tel.: +40.753.081.851
E-mail: siar@siar.ro
VAT Number/CIF 5496135
www.siar.ro
https://www.facebook.com/SIAR.FISITA/
https://www.linkedin.com/company/siar-ro
https://www.linkedin.com/groups

TIPAR
S.C. ART LINES GROUP LTD S.R.L.
Str. Oastei nr. 21,
Bucureşti

The authors declare that the material being presented in the papers is original work, and does not contain or include material taken from other copyrighted sources. Wherever such material has been included, it has been clearly indented or/and identified by quotation marks and due and proper acknowledgements given by citing the source at appropriate places. The views expressed in the articles are those of the authors and are not necessarily endorsed by the publisher. While every case has been taken during production, the publisher does not accept any liability for errors that may have occurred.

EXEMPLAR GRATUIT

SOCIETATEA INGINERILOR DE AUTOMOBILE DIN ROMÂNIA

Cunoaştere şi dezvoltare, prin cooperare! Knowledge and Development by Cooperation!

Preşedinte: Prof. dr. ing. **Nicolae BURNETE**, Universitatea Tehnică din Cluj-Napoca
Vicepreşedinte: Conf. dr. ing. **Victor CEBAN,** Universitatea Tehnică a Moldovei din Chişinău
Vicepreşedinte: Prof. dr. ing. **Anghel CHIRU**, Universitatea „Transilvania" din Braşov
Vicepreşedinte: Prof. dr. ing. **Adrian-Constantin CLENCI**, UNSTP Bucureşti
Vicepreşedinte: Prof. dr. ing. **Ilie DUMITRU,** Universitatea din Craiova
Vicepreşedinte: Conf. dr. ing. **Marius - Florin TOMA** – UNSTP Bucureşti
Vicepreşedinte: Prof. dr. ing. **Bogdan-Ovidiu VARGA**, Universitatea Tehnică din Cluj-Napoca
Secretar General: Prof. dr. ing. **Minu MITREA**, Academia Tehnică Militară „Ferdinand I" din Bucureşti

COMITETUL ŞTIINŢIFIC

Prof. **Dennis ASSANIS**
University of Delaware, DE; National Academy of Engineering, United States of America

Prof. **Rodica A. BĂRĂNESCU**
National Academy of Engineering, United States of America

Prof. **Nicolae BURNETE**
Universitatea Tehnică din Cluj-Napoca, România

Prof. **Giovanni CIPOLLA**
Politecnico di Torino, Italy

Dr. **Felice E. CORCIONE**
Engines Institute, Naples, Italy

Prof. **Georges DESCOMBES**
Conservatoire National des Arts et Metiers de Paris, France

Prof. **Cedomir DUBOKA**
University of Belgrad, Serbia

Prof. **Pedro ESTEBAN**
Institute for Applied Automotive Research, Tarragona, Spain

Eng. **Eduard GOLOVATAI-SCHMIDT**
Schaeffler AG & Co. KG Herzogenaurach, Germany

Prof. **Mircea OPREAN**
Universitatea Naţională de Ştiinţă şi Tehnologie Politehnica din Bucureşti

Prof. **Nicolae V. ORLANDEA**
University of Michigan at Ann Arbor, MI, United States of America

Prof. **Pierre PODEVIN**
Conservatoire National des Arts et Metiers de Paris, France

Prof. **Andreas SEELINGER**
Institute of Mining and Metallurgical Machine, Engineering, Aachen, Germany

Prof. **Ulrich SPICHER**
Kalrsuhe University, Karlsruhe, Germany

Prof. **Cornel STAN**
West Saxon University of Zwickau, Germany

Prof. **Dinu TARAZA**
Wayne State University, MI, United States of America

Prof. **Michael BUTSCH**
University of Applied Sciences, Konstanz, Germany

COMITETUL DE ONOARE AL SIAR

AKA Automotiv – **Mihai - Marin ŞTIROSU**
AVL România – **Thomas SCHEUCHER**
Registrul Auto Român – RAR – **Mihai ALECU**
Uniunea Naţională a Transportatorilor Rutieri din România – UNTRR – **Radu DINESCU**

COLEGIUL DE REDACŢIE

Editor in Chief
Professor *Cornel STAN*
West Saxon University of Zwickau, Germany
E-mail: *cornel.stan@fh-zwickau.de*

Technical and Production Editor
Professor *Minu MITREA*
Military Technical Academy, Bucharest, Romania
E-mail: *minumitrea@yahoo.com*

Contributors:
Anghel CHIRU
George CREANGĂ
Andreeas - Marco FĂRCAŞ
Mariana ILIE
Daniel - Tiberiu IONIŢĂ
Nicolae ISPAS
Dorin LELEA
Minu MITREA
Daniel-Levente NAGY
Gabriel PRUNEAN
Dan - Ştefan SANDOR
Virgil STOICA
Dragoş - Daniel TRUŞCĂ
Daniela VOICU

Registrul SIAR de referenţi ştiinţifici / SIAR register of scientific reviewers:

Horia BELEŞ
Liviu BOCÎI
Alexandru BOROIU
Salvadore-Mugurel BURCIU
Alexandru CERNAT
Adrian-Constantin CLENCI
Valerian CROITORESCU
Radu DROSESCU
Mihai DUGULEANĂ
Ilie DUMITRU
Marius Ioan GHEREŞ
Constantin-Ovidiu ILIE
Sorin ILIE
Ioan LAZA
Dorin LELEA
Marin-Stelian MARINESCU
Liviu-Nicolae MIHON
Lucian MATEI
Minu MITREA
Rodica NICULESCU
Viorel PĂUNOIU
Laurenţiu RĂCILĂ
Adrian-Constantin SACHELARIE
Loreta SIMNICEANU
Ramona-Monica STOICA
Oana-Victoria STĂNCIUC-OŢĂT
Virgil Gabriel TEODOR
Bebe TICĂ
Stelian ŢÂRULESCU
Radu VILĂU
Daniela VOICU

The articles published in „Ingineria automobilului" magazine are indexed by Web of Science in the „Journal Impact FactorTM = 0,4/2025; 0,2 Five Year; Journal Citation IndicatorTM: JCI rIA = 0,04/2025; 0,03/2024 Source: Journal Citation Reports

Web of Science Clarivate Analytics

Articolele publicate în „Ingineria automobilului" sunt incluse în ***Romanian Journal of Automotive Engineering*** *(ISSN 2457 – 5275) – revista SIAR în limba engleză. Revistele SIAR sunt publicate la adresa* ***www.ro-jae.ro***

THE INFLUENCE OF MAGNETIC INSCRIPTIONS APPLIED TO VEHICLES ON ROAD SAFETY AND THE FUNCTIONING OF CAR SENSORS

INFLUENȚA INSCRIPȚIILOR MAGNETICE APLICATE PE VEHICULE ASUPRA SIGURANȚEI RUTIERE ȘI FUNCȚIONĂRII SENZORILOR AUTO

ABSTRACT: *The use of magnetic inscriptions on vehicle bodies – such as authorisation marks, dispatch symbols or identification markings – requires a rigorous analysis of their effects on road safety and the functioning of modern electronic systems. This paper presents a comprehensive study of the aerodynamic, mechanical and electromagnetic behaviour of these elements under real operating conditions. Static and dynamic lift forces, airflow distribution around the bodywork and possible interference with vehicle sensors are evaluated. The experimental results confirm that magnetic inscriptions can disrupt airflow and local magnetic fields, affecting vehicle stability and the functioning of ADAS sensors. The conclusions highlight the need to ban their use on modern and autonomous vehicles, in accordance with the principles of electromagnetic compatibility (EMC).*

REZUMAT: *Utilizarea inscripțiilor magnetice pe caroseria vehiculelor – cum ar fi marcajele de autorizare, simbolurile de expediere sau marcajele de identificare – necesită o analiză riguroasă a efectelor acestora asupra siguranței rutiere și funcționării sistemelor electronice moderne. Acest articol prezintă un studiu cuprinzător al comportamentului aerodinamic, mecanic și electromagnetic al acestor elemente în condiții reale de funcționare. Sunt evaluate forțele de ridicare statice și dinamice, distribuția fluxului de aer în jurul caroseriei și posibila interferență cu senzorii vehiculului. Rezultatele experimentale confirmă faptul că inscripțiile magnetice pot perturba fluxul de aer și câmpurile magnetice locale, afectând stabilitatea vehiculului și funcționarea senzorilor ADAS. Concluziile subliniază necesitatea interzicerii utilizării acestora pe vehiculele moderne și autonome, în conformitate cu principiile compatibilității electromagnetice (EMC).*

Keywords: *Automotive aerodynamics, Magnetic field, Sensors, road safety, Electromagnetic compatibility, Magnetic inscriptions*


Drd. ing.
Daniel-Tiberiu IONIȚĂ
daniel.ionita@unitbv.ro


Prof. dr. ing
Anghel CHIRU


Prof. dr. ing.
Nicolae ISPAS


S.l. dr. ing.
Dragoș-Daniel TRUȘCĂ


Drd. ing.
Gheorghe CREANGĂ

Universitatea Transilvania din Brașov,
Departamentul de Autovehicule și Transporturi,
B-dul Eroilor, Nr. 29, 500024 BRAȘOV, România

1. INTRODUCTION

A main goal of this research is the assessment of the risks generated by the accidental detachment of these signs while driving, with an emphasis on the potential danger of injury to road users, distraction of drivers, or impairment of their visibility.

Given these technical and road safety implications, we consider it necessary to regulate the use of these magnetic inscriptions by requiring a certificate of conformity from the manufacturer. This document should clearly specify the conditions of application (surfaces, positioning, compatibility with body types), the maximum guaranteed period of use, tolerances regarding the holding force, and any precautions regarding influences on the vehicle's electronic equipment.

This scientific paper evaluated the compatibility of inscribed magnetic sheets with the nature of the materials used in the construction of various parts of the bodywork of current motor vehicles. The aerodynamic forces developed on the surfaces to which the inscribed magnetic sheets are attached were studied, as well as the influence of various vehicle speeds on the forces that can cause the magnetic sheets to detach. Valuable conclusions were obtained regarding the electromagnetic compatibility of the sensor system present in a modern vehicle in the presence of magnetic sheets in various areas of the bodywork, and regarding the consequences of accidental detachment of magnetically attached sheets on road safety.

2. ANALYSIS OF THE SHAPE AND AERODYNAMICS OF THE VEHICLE IN INTERACTION WITH MAGNETIC LETTERING SHEETS

To apply the theoretical principles of aerodynamics to a practical case, an analysis of the pressure distribution and air flow behaviour around the body of a production vehicle was carried out. The study aims to highlight areas of stagnation, flow lines and flow separation points that influence the aerodynamic drag coefficient C_x . The vehicle selected for analysis – a 2022 SEAT Ibiza hatchback – is a relevant example for the compact class, providing an adequate basis for correlating geometric characteristics with aerodynamic performance. The theoretical and experimental determination of the *Cx* coefficient contributes to the evaluation of the efficiency of the body shape and to the formulation of conclusions regarding its impact on stability and energy consumption in real operating conditions. The aerodynamic drag coefficient *Cx* is a fundamental parameter in assessing the dynamic performance of a vehicle, expressing the ratio between the drag force and the product of the dynamic air pressure and the frontal area of the bodywork. The general relationship for determining this coefficient is given by the expression [1][2]:

$$C_x = \frac{2F_d}{\rho \cdot v^2 \cdot A} \qquad (1)$$

where: *Fd* - total aerodynamic drag force [N]; ρ - air density [kg/m^3]; v - vehicle speed [m/s];*A* - is the frontal area of the vehicle (m^2).

For the vehicle analysed – SEAT Ibiza, manufactured in 2022, hatchback body – the frontal area is determined by measuring the frontal projection



Figure 1 Magnetic inscriptions applied incorrectly due to the shape of the bodywork.

of the body, and the drag force is estimated based on the speed regime and environmental conditions. The value obtained for the *Cx* coefficient allows the aerodynamic efficiency of the body shape to be assessed and provides useful information on vehicle stability and fuel consumption at different speeds. To determine the approximate value of the aerodynamic drag coefficient *Cx* for the SEAT vehicle, the design data and standard physical parameters corresponding to normal atmospheric conditions were used [3]. Parameters used in equation (1): air density: ρ =1.225 kg/m3 ; estimated frontal area: A =2.05 m2; assumed speed: v =27.78 m/s (equivalent to 100 km/h); Estimated forward resistance force: Fd = 320 N. The value obtained, $Cx \approx 0.40$, falls within the range characteristic of compact class vehicles (0.30 – 0.42), confirming a balanced aerodynamic design. Using [4] we find a $Cx \approx 0.31$ as a real drag aerodynamic coefficient. At speeds above 100 km/h, the influence of the body shape on fuel consumption becomes significant, as aerodynamic drag increases proportionally with the square of the speed. Therefore, optimising design details – such as mirrors, front grille, spoiler or windscreen angle – can reduce *Cx* by 5–10%, leading to lower fuel consumption and improved directional stability. In the case under consideration, the overall shape of the body (hatchback) promotes uniform airflow with limited separation of the flow in the rear area. The angle of inclination of the windscreen and rear window contributes to reducing stagnation pressures. Additional elements, such as crossbars, sign holders or magnetic inscriptions, can increase the *Cx* coefficient by up to 0.02–0.05, affecting stability and energy consumption at high speeds.

3. EVALUATE MAGNETIC LETTERING SHEETS FOR PEELING FORCES

In addition to the theoretical analysis of the influence of shape and size on the aerodynamic behaviour of magnetic inscriptions, presented in the previous chapter, it is necessary to experimentally evaluate their **adhesion force** and **peel resistance** under real operating conditions. This approach is essential in order to correlate the theoretical results (related to additional aerodynamic forces) with the actual behaviour of magnetic materials applied to the surface of a vehicle body, subjected to the combined action of mechanical and environmental factors. The 1.2 mm thick magnetic tape is made of flexible isotropic magnetised rubber, which means that the magnetisation is uniform in all directions [5]. The magnetic tape has magnetic adhesion, attracting ferrous metal objects and allowing easy attachment. It has multipolarity for uniform distribution of the magnetic field over its entire length and is flexible, allowing it to be bent or shaped without losing its magnetic force. However, at low temperatures, its flexibility decreases significantly, making it difficult to adapt to large closing or opening angles and atypical body shapes, thus reducing its effectiveness in curved or irregular areas. As a general recommendation: the steel plate should be ≥15 mm thick for maximum force [5]. If the contact surface is thin, rusty or painted, with moisture and impurities, the force is significantly reduced, even by more than 30%, significantly diminishing the „power" of the magnetic field. Mas and dimensions for magnetic sheets we tested are: total area of inscriptions: 1.24 m2; total weight: 1.984 kg (approximately 2 kg, as adhesive is also applied over it); thickness: 1.25 mm. In daily use, magnetic inscriptions are exposed to variable factors: vibrations, temperature differences, humidity, dust, air currents and turbulence generated by the movement of the vehicle or by encounters with other vehicles travelling in the opposite direction. These factors can lead to reduced adhesion, lifting of the edges or even total detachment, especially when the metal surface is not completely clean or flat. Also, at low temperatures, the flexibility of the magnetic material decreases, which limits its adaptation to the curved shapes of the bodywork, accentuating the tendency to detach (fig. 1).

To evaluate the overall behaviour of these inscriptions, a series of static and dynamic experimental tests were carried out using specialised equipment (digital dynamometer, measuring stands and controlled air flow). These tests aimed to determine the values of the detachment force depending on the type of inscription, surface conditions and angle of force application. The experimental tests were carried out in static and dynamic conditions, using specialised equipment (digital dynamometer, measuring equipment and controlled air flow). These tests aimed to determine the values of the detachment force depending on the type and shape of the inscription, surface conditions and angle of force application. The tests were carried out in a natural environment, at a temperature of 14 ± 2°C and a relative humidity of 50 ± 5%, using the vehicle under test, positioned on a relatively smooth, clean and completely degreased surface. The tests were carried out in two distinct situations: a) clean and dry surface; b) surface with moisture and impurities (thin film of water and fine dust deposits). Each sample was tested in both conditions to determine the variation in adhesion force depending on the condition of the contact surface.

The following equipment and magnetic sheets samples were used to perform the tests:

- AMF-10 digital dynamometer, measuring range 0–200 N (20 kg), accuracy ±0.1%, resolution 0.1 N (0.01 kg), equipped with metal hook and *Peak Hold* function for recording the maximum value;
- Magnetic samples with the following dimensions: thickness/width/length: Type 1 = 1.25 x 185 x 285 mm;

Type 2 = 1.25 x 60 x 1000 mm; Type 3 = 1.25 x 180 x 280 (elliptical shape).

3.1. Determination of static detachment force

To verify the behaviour of magnetic inscriptions under the direct action of forces generated by air currents, a series of **static experimental tests** were carried out with the aim of identifying the moment of **loss of adhesion**, i.e. **the initial, partial and total detachment** from the vehicle body

surface. The tests were designed to reproduce as accurately as possible the actual operating conditions of a moving vehicle subjected to the action of incident air currents and local pressure variations.

The experiments were carried out using an AMF-10 digital dynamometer, a precision instrument used to measure traction force, equipped with a *Peak Hold* function to record the maximum force applied at the moment of detachment. The device was connected via a system of textile wires and fasteners to the upper edge of the magnetic inscriptions to allow for controlled and uniform application of force.

To capture behaviour under various stress conditions, the tests were performed at three distinct angles of force application:

- 90° – traction perpendicular to the surface, simulating direct detachment from the bodywork (vertical pull);
- 45° – oblique traction, combining the lifting and sliding effect, similar to the stress in real airflow conditions;
- 0° - 5° – traction approximately parallel to the surface, equivalent to the direction of airflow over the inscription while the vehicle is moving.

The tests were performed for the three types of magnetic inscriptions (Type 1, Type 2 and Type 3) applied to the side surface of the vehicle, using the AMF-10 digital dynamometer in progressive traction mode. The measurement was performed at angles of 0°, 45° and 90°, under two conditions: clean surface and surface with moisture and impurities. For each case, five measurements were performed, with the maximum value being retained by the *Peak Hold* function of the device. In the first stage of measurements, it was found that the detachment of the tested surface varies gradually depending on the value of the applied force and its angle. The analysis showed that the onset of adhesion loss in the frontal area occurs for forces between 2.7 and 3.8 N, which corresponds to a specific force of 0.146 – 0.20 N/10 mm² under perfectly clean surface conditions. In the case of surfaces with moisture or impurities, the peel force values ranged between 1.3 and 2.1 N, resulting in an equivalent force of 0.07–0.11 N/10 mm². Tests performed on different types of inscriptions were also compared, finding that the initial peel values, measured on the area directly exposed to air currents and the forces generated by them, relative to a surface area of 10 mm², are relatively identical. In order to make a relevant comparison between the results obtained, the total peel strength (for sample T1) was determined under direct force (pull-off type) conditions. The values obtained were as follows: for perfectly clean surfaces: between 14.2 and 15.3 N; for surfaces with moisture or impurities: between 8.1 and 8.6 N. The results obtained highlight the fact that the critical situation is generated by the accumulation of impurities and moisture between the two contact surfaces, a phenomenon that leads to a reduction of approximately half of the stable grip effect and the properties of the magnet. Under these conditions, intense vibrations or mechanical shocks caused by road irregularities can cause the elements to detach accidentally, without this being significantly influenced by the action of air currents [7].

3.2. Determination of the detachment force in dynamic conditions

The practical determination of the additional aerodynamic resistance force on the total area of contact with air currents consists of measuring the actual values of the dynamic pressures generated by the air flow during the movement of the vehicle. This measurement is performed using an anemometer mounted on the side of the bodywork, directly exposed to the airflow, allowing the influence of the design shape on the pressure distribution and total drag force to be assessed. The data obtained is used to validate the theoretical results and to determine the local pressure variations that affect the aerodynamic behaviour of the vehicle in real diving conditions. We calculated the additional aerodynamic drag force using the classic formula [8]:

$$F_d = \frac{1}{2}\,\rho\, C_d\, A\, v^2 \qquad (2)$$

where: F_d - total aerodynamic drag force [N]; ρ - air density, considered to be 1.225 [kg/m³]; Cd - aerodynamic drag coefficient (for thin edges, Cd=2.0); v - vehicle speed [m/s]; A - is the frontal area of the vehicle (m²). Comparative results for the three types of inscriptions (at a speed of v = 27.78 m/s = 100 km/h) are show in the table 1. At the same speed and the same aerodynamic coefficient, the drag force is directly proportional to the exposed frontal area. Comparatively: Type 1 develops a force approximately 3.08 times greater than Type 2 and 10.3 times greater than Type 3; Type 2 produces 3.33 times more drag than Type 3, confirming the geometric advantage of the narrow ellipse. The elliptical inscription (Type 3) mounted correctly has the lowest aerodynamic influence, with minimal contact surface with the air flow. However, if the edges are not perfectly adherent and the magnetic element rises partially, the exposed surface increases significantly (configuration „facing" the flow) [9]. For the 28×18 mm ellipse, in this situation the force increases to F ≈ 0.2058 N, a value comparable to that of the Type 1 inscription, which explains the risk of progressive detachment at high speeds.

Table 1.
Calculated additional force values

Sign type	Frontal area [mm²]	Frontal area [m²]	Additional force [N]
Type 1 (price list)	231.25	2.3125×10^{-4}	0.2186
Type 2 (chess type)	75	7.5×10^{-5}	0.0709
Type 3 (City Hall authorisation)	22.5	2.25×10^{-5}	0.0213

Experimental analysis shows that small magnetic inscriptions, especially those with elliptical geometry (Type 3), have a minimal aerodynamic influence on the airflow around the vehicle, provided they are correctly applied to smooth, dry and clean surfaces of the bodywork [10].

On the other hand, improper application – on wet, contaminated or locally rough surfaces – increases drag force due to boundary layer disruption and micro-vibrations induced by air currents. These phenomena contribute to a decrease in magnetic adhesion and can cause partial or total detachment of the inscription under dynamic conditions.

The effect is amplified at low temperatures, when the flexibility of the magnetic material is reduced and the internal stresses in the ferromagnetic layer increase, favouring the formation of microscopic gaps at the contact interface, causing their accidental detachment [11].

3.3. Practical determination of the additional force (aerodynamic force) of resistance in the total area of the surface in direct contact with air currents.

The practical determination of the additional aerodynamic resistance force on the total area in contact with air currents consists of measuring the actual values of the dynamic pressures generated by the air flow during the movement of the vehicle. This measurement is performed using an anemometer mounted on the side of the bodywork, directly exposed to the airflow, allowing the influence of the design shape on the pressure distribution and total drag force to be assessed. The data obtained is used to validate the theoretical results and to determine the local pressure variations that affect the aerodynamic behaviour of the vehicle in real driving

conditions. Analysis of the accidental detachment of magnetic inscriptions as a function of airflow velocity - the process of accidental detachment of magnetic inscriptions applied to the surface of the vehicle body under the action of airflows generated in a controlled regime is analysed. The air flow velocity was determined using the Testo 417 digital anemometer, an instrument designed to measure flow velocities and air flow rates within its operating range. Given that the Testo 417 anemometer can measure air speeds of up to approximately 70 km/h (≈ 19.4 m/s), for higher speeds, values were estimated based on the variation trend of the results obtained within the measurable range. Thus, a series of measurements were taken at speeds of 10 km/h, 20 km/h, 30 km/h, 40 km/h, 50 km/h, 60 km/h and 70 km/h, and values above this limit were extrapolated by analysing the behaviour of the experimental curves until the effective separation speed was reached.



Figure 2. Air speed and volumetric flow measurement.

The tests yielded magnetic marking separation values between 91 and 118 km/h at a temperature of 14°C. Analysis of the experimental data showed that the onset of loss of adhesion was observed at speeds approximately 5 km/h lower than the values indicated in the previous table.

3.4. Analysis of detachment caused by the airflow generated by a vehicle travelling in the opposite direction

Critical situation – interaction of air currents between vehicles travelling in opposite directions. To assess the dynamic behaviour of magnetic inscriptions in real traffic conditions, a controlled test was carried out on a straight road in the Rădulești area, Vrancea County. The experiment monitored the critical moment of detachment (T2) in relation to weather conditions and wind direction, recorded in real time. The data was correlated with vehicle speed, atmospheric pressure and the direction of the prevailing air flows to determine the influence of environmental parameters on the stability of the markings. In real traffic conditions, the accidental detachment of magnetic inscriptions is not determined

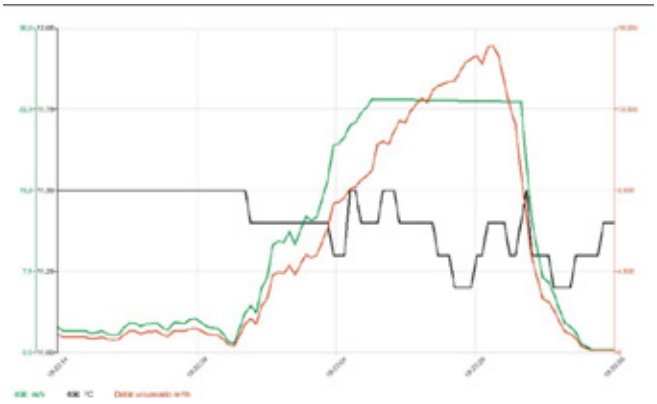


Figure 3. Reference diagram of values with air current speed, volumetric flow

Table 2.
Values obtained from dynamic tests

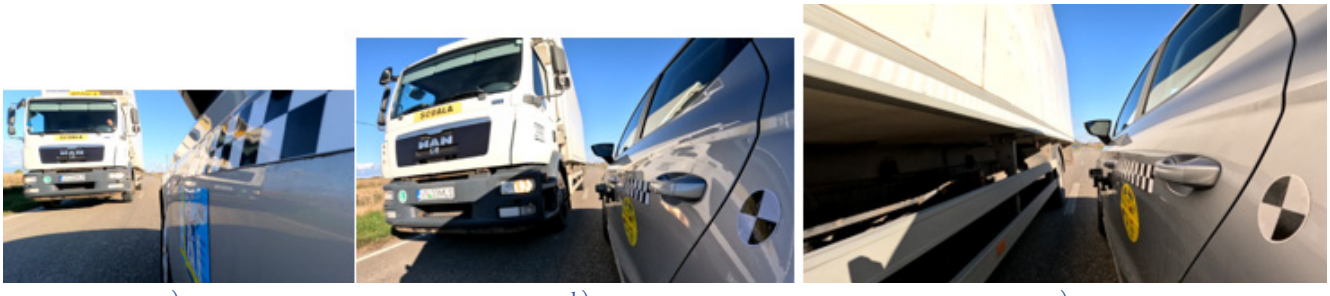
Cleaned surfaces	Wet surfaces with impurities	Air current speed	Temperature
113...115 km/h	91 ... 94 km/h	102 ....108 km/h	12° C

exclusively by the vehicle's own speed, but also by the complex interaction of air currents generated by vehicles moving in different directions. These phenomena, known as aerodynamic vortices or aerodynamic interaction currents, create critical situations for the mechanical stability of magnetic inscriptions applied to the bodywork [11].

When two vehicles (a heavy goods vehicle and a passenger car) meet, the air displaced by each produces areas of positive and negative pressure. When these areas overlap, sudden pressure variations and local turbulent flows occur, which can generate instantaneous detachment forces on the magnetic inscriptions. The critical and detachment area was identified at the end of the rear console.

Following the tests carried out, it was observed that the adhesion of magnetic inscriptions is significantly influenced by the condition of the contact surface between the metal support and the magnetic material. The presence of moisture, dust or other impurities causes the formation of a contaminant layer that reduces magnetic attraction forces and promotes slippage or partial detachment of the inscriptions during vehicle movement. These effects are amplified under dynamic conditions, when air flows contribute to the formation of variable pressure zones. During the dynamic test, the critical moment of total detachment of the magnetic inscriptions was observed, generated by the combination of lateral turbulence and sudden pressure variations caused by the proximity of the compact body of the truck [12].

In this phase, the aerodynamic effects reach their maximum intensity, and



a) b) c)

Figure 4. Sequence of the test for resistance to detachment of magnetic inscriptions in the vicinity of a large vehicle (a.- initial approach of the test vehicle to the reference lorry, b.- passage of the test vehicle through the area of turbulence generated by the lorry; c.- complete lateral alignment and verification of the stability of the magnetic inscriptions)

the layer of negative pressure air formed between the two vehicles acts directly on the upper edge of the magnetic inscription. The phenomenon indicates a complete loss of magnetic adhesion, confirming the decisive influence of compressed air flows and dynamic travel conditions (figure 4).

4. ANALYSIS OF THE MAGNETIC FIELD GENERATED BY MAGNETIC LETTERING AND THE POTENTIAL IMPACT ON MODERN AND AUTONOMOUS VEHICLE SENSORS

The rapid development of automotive technologies over the last decade has led to an exponential increase in the degree of electronation and sensitization of vehicles. Modern driver assistance systems (ADAS), radar and *lidar* sensors, and proximity data processing units are now essential components for safety and the operation of autonomous vehicles. In this context, the application of flexible magnetic lettering on vehicle bodies — a common practice in advertising or commercial transport — can represent an electromagnetic risk factor. These elements, although seemingly harmless, generate static magnetic fields with intensities in the order of tens of micro-Tesla (μT), sufficient to interfere with field detection and measurement sensors, especially in sensitive areas of the vehicle (bars, doors, bonnet or rear window) [13]. The purpose of this chapter is to highlight the potentially disruptive effects of the magnetic fields generated by these inscriptions and to argue for the need to ban their use on modern and autonomous vehicles to protect the integrity of active and passive safety systems. To assess the intensity of the magnetic field generated by magnetic inscriptions, an FNIRSI ERD-10 electromagnetic radiation detector was used, a highly sensitive portable instrument capable of measuring static magnetic fields and low-frequency electromagnetic fields, with a measurement range of 0.01–200 μT, with an accuracy of ±0.4 μT, frequency range 50 Hz – 3.5 GHz.

The measurements were performed by positioning the FNIRSI ERD-10 detector perpendicular to the geometric centre of each inscription. The measurement distances were: 1 cm, 5 cm, 10 cm, 20 cm and 50 cm from the surface (Table 3).

Table 3.
Magnetic field intensity values as a function of distance

Distance from the inscription (mm)	Average magnetic field intensity (μT)	Observations
10	81.7	Strong static field, specific to permanently magnetised materials
50	27.8	Rapid decrease in field intensity
100	17.8	Low but detectable level
200	9.6	Weak but persistent field
300	3.5	Weak but persistent field
500	<1.0	Below the instrument's detection limit

5. CONCLUSION

The research aimed to analyse the behaviour of magnetic markings applied to vehicles from the perspective of road safety, aerodynamic stability and electromagnetic compatibility.

The experimental results highlighted several key aspects:

1. The static detachment force determined with the AMF-10 digital dynamometer demonstrated that the adhesion of magnetic inscriptions depends significantly on the condition of the contact surface.
2. On clean and dry surfaces, the detachment forces are high, providing relatively stable fixation.
3. In the presence of moisture, impurities or fine dust, the adhesion force decreases by up to 30–40%, which increases the risk of accidental detachment in traffic.
4. The aerodynamic interaction between air currents generated by vehicles travelling in opposite directions produces vortices and turbulence that can cause signs to detach even at moderate speeds.
5. Tests conducted between a truck travelling at 90 km/h and a test vehicle equipped with magnetic lettering have shown that detachment frequently occurs at combined speeds equivalent to 120–130 km/h.
6. These phenomena are more intense on the sides and rear of vehicles, where interaction currents are unstable.
7. Determination of the magnetic field of the inscriptions indicated values between 70–85 μT at contact, decreasing below 10 μT at 10 cm. Although these values are relatively small, they can disrupt the electromagnetic sensors used in modern assistance systems (ADAS), positioning systems and autonomous vehicles.
8. With the increasing density of electromagnetic and radar sensors on vehicles, even weak static magnetic fields can induce calibration errors, false alarms or interference in communication between subsystems. Therefore, the use of magnetic inscriptions on modern vehicles contravenes the principles of electromagnetic compatibility (EMC) and may affect active safety.
9. From a physical integrity perspective, magnetic inscriptions also pose secondary risks: detachment in traffic, with the potential to hit other vehicles; degradation of bodywork finishes due to the accumulation of dust and moisture under the magnetic layer; reduced visibility of optical and radar sensors if applied in critical areas.

REFERENCES:

[1] Sumantran, V., Sovran, G. – Vehicle Aerodynamics, SAE International, PT-49, Warrendale, USA, 1990.
[2] Cembalo, E. – Trainee en Aérodynamique Automobile, European School of Mechanical Engineering (ESMA), 2024.
[3] Popescu, M., Bădescu, A., Dima, I. – Aerodynamics of Motor Vehicles, Polytechnic University of Bucharest Publishing House, 2011.
[4] Specs for all Seat Ibiza 2022 versions https://www.ultimatespecs.com/car-specs/Seat/M11961/Ibiza-2022
[5] https://www.decals.com/oem-manufacturing
[6] Mirmahdi E., Karimi M. H., Khoubrou K, Sajed S. A. - The Effect of Aerodynamic Forces on Automotive
Design and Reducing Fuel Consumption – International Journal of Robotics and Automation, Volume 7, Issue 1, 2021 DOI (Journal): 10.37628/IJRA
[7] Popescu, M. (coord.) – Aerodynamics of Motor Vehicles – University Course, Polytechnic University of Bucharest, available at: https://www.scribd.com/document/559102619/11-Aerodinamica-autovehiculelor, accessed on 11.10.2025.
[8] Hucho, W.-H. – Aerodynamics of Road Vehicles: From Fluid Mechanics to Vehicle Engineering, 5th Edition, SAE International, Warrendale, 2013.
[9] Barnard, R. H. – Road Vehicle Aerodynamic Design: An Introduction, Mechaero Publishing, 2011.
[10] Katz, J. – Race Car Aerodynamics: Designing for Speed, 2nd Edition, Bentley Publishers, 2016.
[11] Wood, D. – Automotive Aerodynamics, Elsevier Butterworth-Heinemann, 2019.
[12] Tanaka, Y., Nakamura, K. – „Electromagnetic Interference Between Magnetic Vehicle Decals and Autonomous Vehicle Sensors", IEEE Transactions on Vehicular Technology, Vol. 71, No. 8, 2022.

D110 DIESEL ENGINE–BASED COGENERATION SYSTEM FOR ELECTRIC MOBILITY AND RESIDENTIAL HEATING

SISTEM DE COGENERARE CU MOTOR DIESEL D110 PENTRU MOBILITATE ELECTRICĂ ŞI ÎNCĂLZIRE REZIDENȚIALĂ

ABSTRACT: *The present paper proposes the development of a cogeneration system based on the D110 diesel engine that provides electricity and heat for households while also supporting and encouraging electric mobility. The diesel engine, originally used in the U650 Romanian tractor, is still widely used today in rural areas of the country. It was chosen for its flexibility in using a wide variety of fuels, easy maintenance, and well-known production technology, in use since the 1960s. The proposed system can produce about 40 kW of electricity and 75 kW of heat, with an overall efficiency of about 84–90%. When paired with a heat pump, the "thermal efficiency" can easily reach 140–150%, due to the additional heat pumped from the environment. Complementing the photovoltaic system with such a cogeneration system and electric vehicles can lead to a much more efficient thermo-electric household system, also covering the household owner's mobility needs.*

REZUMAT: *Lucrarea de față propune dezvoltarea unui sistem de cogenerare bazat pe motorul diesel D110, destinat locuințelor, care furnizează energie electrică și termică, susținând și încurajând în același timp mobilitatea electrică. Motorul diesel D110, care a echipat tractorul românesc U650, este încă foarte utilizat în zonele rurale ale țării. A fost ales datorită capacității sale de a funcționa cu o gamă largă de combustibili, întreținerii ușoare și tehnologiei de fabricație bine cunoscute, fiind produs încă din anii '60. Sistemul propus poate genera aproximativ 40 kW electrici și 75 kW termici, cu o eficiență globală de circa 84–90%. Atunci când este cuplat cu o pompă de căldură, „eficiența termică" poate ajunge ușor la 140–150%, datorită căldurii suplimentare preluate din mediul ambiant. Combinarea acestui sistem de cogenerare cu un sistem fotovoltaic și cu vehicule electrice poate conduce la un sistem termo-electric eficient pentru locuințe, acoperind totodată și nevoile de mobilitate ale utilizatorului.*

Keywords: *electric mobility, cogeneration, ICE, renewable fuels, heat pump*



Conf. dr. ing.
Virgil ȘTOICA [1)]



Conf. dr. ing.
Mariana ILIE [2)]
mariana.ilie@upt.ro

1) Universitatea Politehnica din Timișoara, Departamentul de Mașini Mecanice, Utilaje și Transporturi, Str. Mihai Viteazul, Nr. 1, 300222 TIMIȘOARA, România
2) Universitatea Politehnica din Timișoara, Departamentul de Mecatronică, Str. Mihai Viteazul, Nr. 1, 300222 TIMIȘOARA, România

1. INTRODUCTION

In the current context, marked by rising energy prices, the shift from conventional to electric propulsion in transportation, the need to transition from fossil fuels to renewable energy sources, and the increasing number of solar energy prosumers, it is necessary to develop an integrated energy system capable of meeting the energy demands of a household, including transportation needs. Most households, especially in rural Romania, use traditional, low-efficiency heating systems based on wood, biomass, coal, or gas. Only a few households currently have photovoltaic systems for electricity generation, although their number is increasing. To increase the overall efficiency of these three energy systems, which currently operate independently and do not complement each other, an integrated energy approach is necessary and is proposed in this paper. Integrating the electric road vehicle into the household energy system is necessary for two reasons. First, the car can be charged with low-cost electric energy during the whole year and, second, the car can serve as a household energy storage system.

In Romania, solar activity is sufficient to enable a household to produce, during spring and summer (approximately seven months per year), enough electricity to cover all domestic needs, including charging electric vehicles, with a surplus that can be fed back into the grid. However, during autumn and winter, the electricity produced may only partially cover the household's electrical demand, and sometimes not even that. At the same time, the demand for thermal energy significantly increases during this period. Therefore, by integrating a cogeneration system based on a thermal engine operating on renewable or conventional fuels, it is possible to achieve household energy independence, including transportation needs, with higher efficiency and lower costs.

A techno-economic study [1] has shown that cogeneration systems can become profitable in less than 15 years, even when using costly technologies such as Stirling, gas engines or biomass-based ORC systems. Among the technologies evaluated, internal combustion engine systems proved to be the most cost-effective for prosumers [2], thanks to their low costs and operational flexibility with a wide range of fuels, from methane gas and LPG to vegetable oils and biogas [3]. It should be considered that the analyses were done when using the cogeneration system by itself and not complemented by a photovoltaic system.

Cogeneration, by simultaneously producing heat and electricity, can achieve thermal efficiencies of up to 140–150% when the electricity is

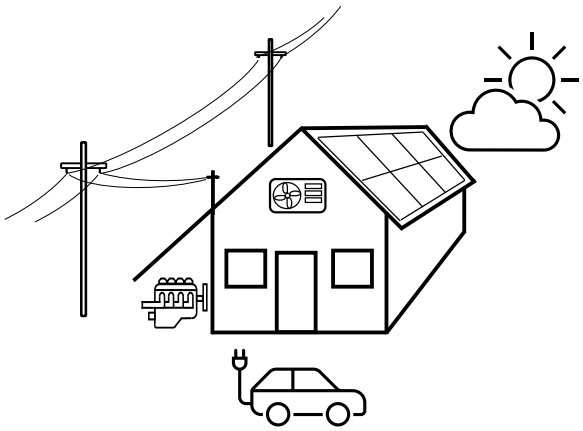


Figure 1. Main components of a household thermo-electric system: cogeneration unit with internal combustion engine, heat pumps, photovoltaic panels, and electric vehicle

used to power heat pumps. Recovering the wasted heat from thermal engines [4] is crucial for improving overall system efficiency, either by generating additional electricity [5], using it in various technological processes [6], or for heating and hot water preparation. The exclusive use of internal combustion engines for electricity generation is considered inefficient, as is its use only for transportation.

Vegetable oils represent a promising source of renewable fuel, with positive outcomes in their use for heating and hot water production [7][8]. Experiments with vegetable oils and biodiesel, either in pure form or mixed with diesel, have shown variations and contradictions regarding engine performance and emissions, requiring further investigation for clarification [9][10][11][12][13][14]. It is worth noting that using vegetable oil can reduce engine lifespan [15]. The negative effects, depositions within the combustion chamber, of using biodiesel in diesel engines, are noticed also by other researchers [16], who propose, at the same time, the usage of additives as countermeasures. The alternative fuels and blends also affect the characteristics of the lubrication oil [17], leading to a reduced engine lifespan. All these negative effects, we suppose, are more pronounced in road traction applications where the engine frequently operates at low load and speed regimes.

The advantages of using vegetable oils and biodiesel include contributions to the local economy, biodegradability, renewability, low sulfur content, and a higher flash point compared to diesel, making them safer to handle [7][8]. Cogeneration systems are increasingly produced and utilized on a larger scale, particularly those operating on gas. Since the 2010s, studies have highlighted the advantages of cogeneration systems using vegetable oil, and manufacturers of such systems already exist. However, these systems are generally expensive, and most of the population in Romania would not be able to afford them. In conclusion, current research highlights the significant potential of cogeneration systems based on renewable fuels in addressing energy and environmental challenges. However, a more detailed analysis of the efficiency and long-term sustainability of these systems is required to maximize their benefits in the global transition to cleaner and renewable energy sources.

This paper aims to present the concept and the design of a cogeneration group that operates on fuels obtained from renewable sources, which will be accessible and affordable for the rural population of Romania, easy to maintain, and simple to operate. For this purpose, the D110 Romanian engine used in the U650 tractor, widely distributed, and still used in rural areas of Romania, will be employed. It is a robust engine with high reliability, based on known manufacturing technology, for which all components are still produced, and the cost is low. Being an engine used in agriculture since the 1960s and still present, its operation and maintenance procedures are well known among the rural population, and the maintenance costs are very low. In this context, the system will be easily accepted by the rural community. Although the lifespan of the main components is very long, this engine is fully recyclable.

The cogeneration unit would produce approximately 40 kWe (electrical power) and 75 kWt (thermal power), with an estimated overall efficiency of 85–90%. The cogeneration unit is designed for use during cold periods when the demand for thermal energy is high. Integrating this unit into a comprehensive thermos-electric system, which includes both photovoltaic panels and thermal and electrical storage solutions, can provide year-round energy autonomy for a variety of households, institutions, and locations, including transportation needs. This approach ensures a consistent and sustainable energy supply, even under varying weather conditions and energy demands. Pairing the cogeneration unit with a heat pump could result in thermal efficiencies of about 140–150%, highlighting the system's superior efficiency. Primarily aimed at rural and peri-urban areas with limited access to traditional energy resources, the use of local biofuels and renewable energy resources promotes energy independence and reduces CO_2 emissions.

2. DESIGN CONCEPT OF A D110 ENGINE-BASED COGENERATION SYSTEM

The cogeneration group, schematically presented in Figure 1, consists of the interconnection of three subsystems:

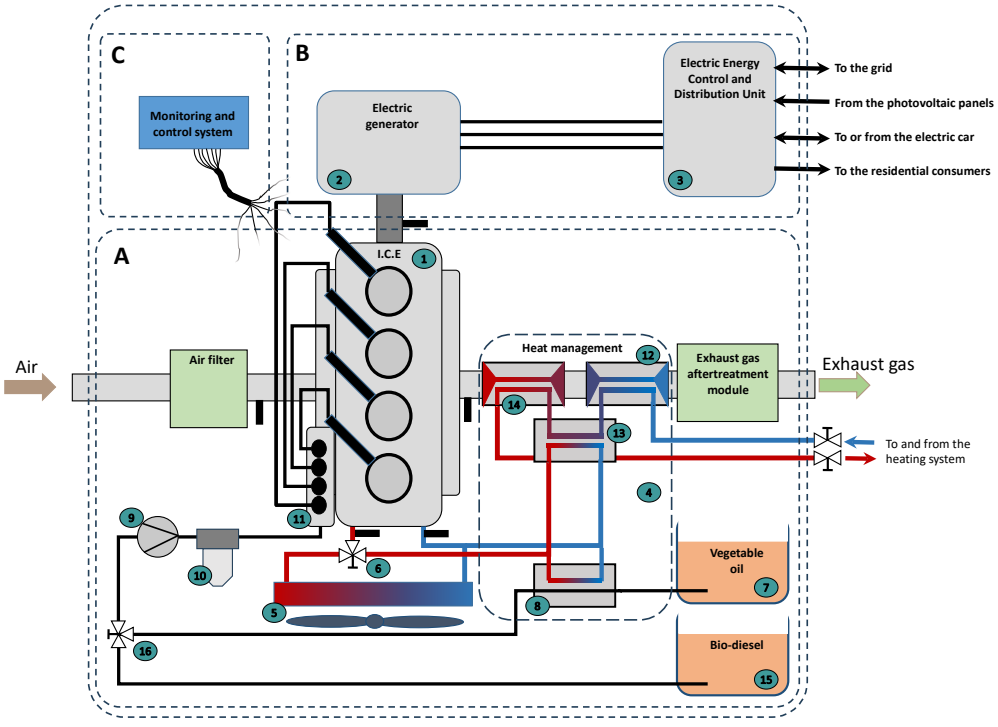


Figure 2. Schematic diagram of the cogeneration group

A. A thermo-mechanical energy system including an internal combustion engine with necessary auxiliary equipment and a thermal module composed of heat exchangers for heat recovery and distribution.
B. An electro-energy system made up of an electric machine (electric generator), an energy control and distribution unit, and necessary auxiliary systems for interconnection.
C. A management and control system featuring an electronic control unit, sensors, and actuators, ensuring monitoring, control, diagnostics, and connection to an integrated energy management system.
The compression-ignition internal combustion engine 1, of D110 type, operating at 1500 RPM, drives an electric generator 2 connected to the AC three phase grid. For connecting with other energy sources or to provide energy to some consumers the inverter included in the photovoltaic system will be used.
The heat generated by the internal combustion engine is captured by thermal module 4 and distributed to consumers. This module consists of a series of heat exchangers that efficiently recover heat of varying quality produced by the engine. It includes two liquid-liquid heat exchangers 13 for recovering the heat dissipated through the engine's cooling system, and 8 for heating the fuel, and two gas-liquid heat exchangers 12 and 14 for exhaust heat recovery. An additional heat exchanger 5 is designed to prevent engine overheating when there's a demand for electrical energy but not for thermal energy. The switch between the two cooling circuits is managed by a three-way thermostat 6.
The engine is powered by vegetable oil or heavy fuel oil from tank 7, aided by the low-pressure pump 9, with the fuel then passing through filter 10 to the injection pump 11. Researchers [11] suggest starting the engine on biodiesel and warming it to operational temperature before switching to vegetable oil to prevent deposit formation in the combustion chamber, and to switch back to biodiesel before shutdown to cleanse the injection system, thus extending engine life. Consequently, an additional biodiesel tank 15 and a solenoid valve circuit 16 are used for automatic switching between vegetable oil or heavy fuel oil and biodiesel or diesel. All three subsystems are mounted on a chassis equipped with a protective, thermally and acoustically insulating casing. This diesel-powered engine reaches a maximum power of 65HP at 1800 RPM. Within the cogeneration system, it operates at 1500 RPM, generating 44kW of power with a diesel consumption rate of 11.34kg/h. Considering the fuel's lower heating value of 42 MJ/kg, the potential input power is approximately 132 kW. The expected thermal and electrical outputs align with the Sankey diagram in Figure 3.

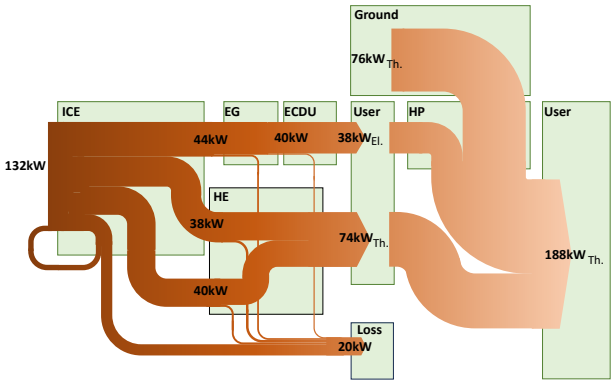


Figure 3. Sankey energy flow diagram. ICE-internal combustion engine, EG – electric generator, ECDU – electricity conversion and distribution unit, HP – heat pump, HE – heat exchangers

As mentioned, the D110 engine, used in the project, is the successor to the D103 engine, differing only in valve timing. The research [18], conducted at the University Politehnica Timisoara's internal combustion engine laboratory, demonstrated the D103's versatility, efficiently operating even with heavy fuel oil, with minor performance drops. These can be improved through optimized adjustments and functional parameter tuning as the author of the research pointed out. The engine D103 was also characterized [19] from the emissions point of view, when running with diesel and rapeseed oil blends. Further experiments with the D110 showed the feasibility of dual fueling this diesel engine with diesel and LPG [20], expecting similar functionality with vegetable oil and biogas mixtures. Hydrogen is also considered as a future potential promising fuel for diesel engine [21]. Studies [22] on diesel engines dual-fueled with diesel and alcohol showed promising results, achieving up to 30% substitution while maintaining or even enhancing engine performance in some regimes [23][24]. Moreover, diluted alcohol injection in diesel engines and water injections in gasoline engines have shown reduction in nitrogen oxide emissions [25]. All this shows the D110 diesel engine's potential for efficient operation with a wide range of fuels, including more eco-friendly options, thus providing a solid foundation for its use in the cogeneration project. Since the costs of the produced energy are important when choosing one solution or another, Figure 4 presents a comparison of the electric and thermal energy produced by the proposed system and the market prices for the same energy.
For the calculations, the Sankey diagram from Figure 3 was considered, together with the fuel costs on the market [26] and, as reference, the market electric and thermal energy prices [27][28].
Since electric energy is more expensive, being a higher-quality energy type than thermal energy, the calculations were performed considering that the produced electric energy is three times more expensive than the thermal one.
Figure 4 presents the electricity and heat prices obtained with the current system when operating with different fuels. The blue and orange bars represent the specific prices of electricity and heat. The horizontal shaded areas indicate the market price ranges, where the pink band corresponds to heat obtained by natural gas combustion, while the blue band represents the electricity market price.

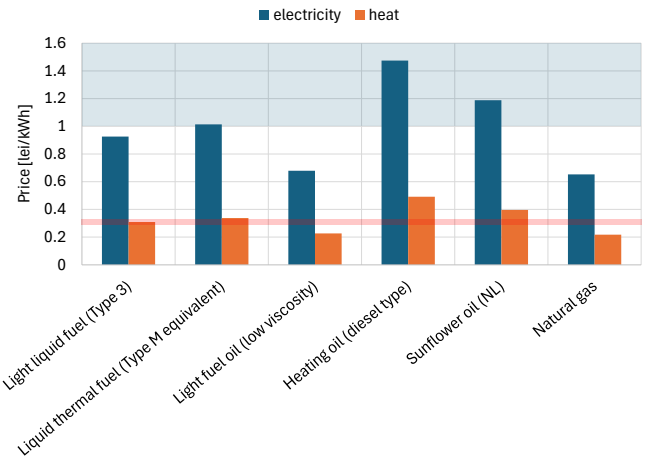


Figure 4. Specific electricity and heat production prices for different fuel types compared to market prices

5. CONCLUSION

The present paper highlights the advantages of integrating an internal combustion engine into a household energy system. Such an integrated approach can provide a significant level of energy independence by simultaneously covering both domestic and transportation energy needs. In the proposed system, the Romanian D110 diesel engine was selected due to its robustness, the widespread availability of parts, and the familiarity of its manufacturing and maintenance procedures among the Romanian population. Additionally, the engine has demonstrated high operational flexibility, being capable of running on a wide range of renewable fuels and fuel blends.

By complementing a photovoltaic energy system with a cogeneration unit based on the D110 engine, the thermo-electric demands of a household can be met throughout the entire year, including those related to electric vehicle charging. Depending on the selected fuel, the total energy cost of such a system can be comparable to, or even lower than, energy prices offered by private suppliers, and in some cases similar to natural gas costs. A major advantage of integrating cogeneration into the household energy system is the possibility of coupling it with a heat pump, which can increase the overall thermal efficiency to values exceeding 140%. This is a significant improvement compared to conventional boilers, which convert the chemical energy of the fuel, only into heat and do not utilize the full energetic potential of the combustion process. In contrast, cogeneration provides both electricity—considered a superior and more valuable form of energy—and heat, maximizing fuel utilization.

However, instead of using the internal combustion engine inefficiently onboard the vehicle—where it operates most of the time under transient and suboptimal conditions, especially in urban driving—it is relocated to a stationary cogeneration unit. In this configuration, the engine remains available for mobility by supplying the electric energy required to charge the vehicle, but it operates in a controlled environment, at steady-state regimes close to its optimal efficiency. At the same time, the thermal energy that would normally be wasted through the exhaust and cooling systems in automotive applications is fully recovered and used to cover the heating demand of the household. In addition, stationary operation removes design constraints typical for vehicles, such as weight, space, or packaging limitations, enabling the use of robust components, higher capacity aftertreatment systems, and improved combustion strategies. Therefore, this approach does not eliminate the internal combustion engine but rather integrates it into a more efficient energy architecture, aligned with current sustainability and energy efficiency objectives.

REFERENCES:

[1] Atanasoae, P., *Technical and Economic Assessment of Micro-Cogeneration Systems for Residential Applications*, Sustainability, vol. 12, p. 1074, 2020.

[2] Sztekler, K.; Siwek, T.; Kalawa, W.; Stefanski, S.; Surowiec, T. and T. M. Wojcik, *Potential uses of small cogeneration systems in prosumer systems*, IOP Conf. Series: Earth and Environmental Science, 2019.

[3] Krawczyk, D., A., Buildings2020+,Energy Sources, Vilnius: Bialystok - Cordoba, 2019.

[4] Brezani, M.; Labuda, R.; Barta, D. and Repka, J., *Using of waste heat of internal combustion engine*, XXII International Scientific-technical conference „trans&MOTAUTO '14", 2014.

[5] Kabeyi, M., J., B. and Olanrewaju, O., A., *Cogeneration potential of an operating diesel engine power plant*, Energy Reports, vol. 8, pp. 744-754, 2022.

[6] Olmos-Villalba, L.; Herrera,B.; Gallego, A. and Cacua, K., *Experimental Evaluation of a diesel cogeneration system for producing power and drying aromatic herbs*, Sustainability, vol. 11, p. 5121, 2019.

[7] Alonso, J., F., S., J.; Sastre, J., A., L.; Romero-Avila, C., R., E., L. and Iglesias, C. I., *Using mixtures of diesel and sunflower oil as fuel for heating purposes in Castilla y Leo´n*, Energy, vol. 30, pp. 573-582, 2005.

[8] Mihaescu, L.; Oprea, I.; Negreanu, G. and Popescu, R., *Combustibili vegetali pentru producerea de energie termica in mediul rural*, Revista Constructiilor, vol. decembrie, 2008.

[9] Can,O., *Combustion characteristics, performance and exhaust emissions of a diesel engine fueled with a waste cooking oil biodiesel mixture*, Energy Conversion and Management, vol. 87, pp. 676-686, 2014.

[10] Hirkude, J. and Padalkar, A., S., *Experimental investigation of the effect of compression ratio on performance and emissions of CI engine operated with waste fried oil methyl ester blend*, Fuel Processing Technology, vol. 128, 2014.

[11] Sidibe,S., S.; Blin, J.; Vaitilingom, G. and Azoumah, Y., *Use of crude filtered vegetable oil as a fuel in diesel engines state of the art: Literature review*, Renewable and Sustainable Energy Reviews, vol. 14, 2010.

[12] Arapatsakos,C.; Karkanis, A.; Cristoforidis, D. and Mitroulias, D., *Sunflower oil as fuel in a diesel engine*, WIT Transactions on The Build Environment, Urban Transport XIV, vol. 101, 2008.

[13] Benea, B., C. *Emissions characteristic of diesel engine fueled by biodiesel at partial load*, Ingineria automobilului, vol. 48, no. Septembrie, 2018.

[14] Banari, E. and Mancuș, N., *Environmental impact of biofuels*, Ingineria automobilului, vol. 45, pp. 14-15, 2017.

[15] *Straight Vegetable Oil as a Diesel Fuel?*," U.S. Department of Energy, Office of Energy Efficiency & Renewable Energy, 2021.

[16] Bâldean, D. and Burnete, N., *Research Possibilities of Biodiesel Combustion in Compression Ignition Engines*, Ingineria Automobilului, vol. 6, no. 1, pp. 16-18, 2012.

[17] Barabás,I.; Todoruț, A. and Băldean, D., *Evaluating the quality of lubricating oil for a compresions ignition engine fueled by diesel-biodiesel-ethanol blend*, Ingineria Automobilului, vol. 13, no. Decembrie-Ianuarie, 2010.

[18] Raica, T., *Contributii la studiul posibilitatilor de ardere a combustibilor grei indigeni in motorul D-103*, PhD thesis, Universitatea Politehnica Timisoara, Timisoara, 1973.

[19] Burciu,S., M.; Lupchian, M. and Neacșu, M., *Reducing CO2 emissions from tractor engines by using the diesel fuel and rapeseed oil blend*, IOP Conference Series: Materials Science and Engineering,The XXII-nd National Conference on Thermodynamics, Galați, 2019.

[20] Molnar,C.; Izvorean, S.; Borborean, A., T. and Stoica,V., *The effect of LPG use over the performance of a diesel engine*, The 33rd SIAR International Automotive and Transportation Engineering Congress, ESFA 2023, Bucuresti, 2023.

[21] Cernat,A.; Negurescu, N.; Nutu, C.; Pana, C.; Fuiorescu, D.; Georgescu, R. and Panait, A., G., *Experimental study of the influence of hydrogen on the combustion in the diesel engine cylinder*, Ingineria Automobilului, vol. 75, no. Iunie, 2025.

[22] Izvorean, Ș. and Stoica, V., *Experimental test bench with diesel engine for the study of multi fuels usage*, IOP Conference Series: Materials Science and Engineering, vol. 1220, no. 1, 2022.

[23] Izvorean, Ș.; Stoica, V. and Lelea, D., *Experimental Research on Dual Fuel Injection System for Diesel-Alcohol Engine*, Heat Transfer Engineering, pp. 1-12, June 2025.

[24] Izvorean, Ș.; Stoica, V. and Lelea, D., *Diesel engines and the palinka from Transylvania. Experimental research*, Ingineria automobilului, vol. 70, pp. 14-17, 2024.

[25] Borborean, A., T.; Stoica, V. and Lelea, D., *Test bench for studying the effects of water injection inside an internal combustion engine*, IOP Conference Series: Materials Science and Engineering, vol. 477, 2019.

[26] E-COMBUSTIBIL, *https://ecombustibil.ro/categorie-produs/combustibil-lichid/*

[27] Selectra, Economisi.ro, *https://economisi.ro/energie/pretul-energiei/pret-energie-electrica*

[28] ENGIE, *engie.ro*

ENERGY EFFICIENCY OPTIMISATION IN AUTONOMOUS VEHICLE POWERTRAIN

OPTIMIZAREA EFICIENȚEI ENERGETICE A SISTEMULUI DE PROPULSIE AL VEHICULELOR AUTONOME

ABSTRACT: *The rising need of autonomous electric vehicles in urban public transport requires the development of cost-effective energy reduction strategies that do not rely on expensive hardware modifications. This paper investigates energy efficiency optimization for an autonomous electric shuttle powertrain by implementing a software-based intelligent acceleration control strategy focused on coasting. The study combines a theoretical analysis of electric powertrain architecture and eco-driving algorithms with a comprehensive simulation implemented via IPG CarMaker and MATLAB-Simulink. The EasyMile EZ10 autonomous shuttle serves as the case study, simulated on a virtual replica of a real-world urban route in Cluj-Napoca. Energy performance is evaluated by comparing four simulation scenarios across speed limits of 30 km/h and 50 km/h, both with and without the proposed optimization strategy. Results indicate energy consumption reductions of approximately 16% at 30 km/h and over 35% at 50 km/h, with minimal impact on travel time. Conclusions demonstrate that software-based driving strategy optimization can significantly enhance the energy efficiency of autonomous urban public transport vehicles, offering a viable solution for sustainable mobility.*

REZUMAT: *Creșterea utilizării vehiculelor autonome electrice în transportul public urban impune dezvoltarea unor strategii eficiente de reducere a consumului energetic, fără a implica modificări hardware costisitoare. Această lucrare investighează optimizarea eficienței energetice a sistemului de propulsie al unui microbuz autonom electric prin implementarea unei strategii software de control inteligent al accelerației, bazată pe rularea liberă (coasting). Studiul combină o analiză teoretică a arhitecturii sistemului de propulsie electric și a algoritmilor de eco-driving cu o implementare detaliată de simulare utilizând platformele IPG CarMaker și MATLAB-Simulink. Ca studiu de caz, este analizat microbuzul autonom EasyMile EZ10, operat pe un traseu urban real din Cluj-Napoca. Performanța energetică este evaluată prin compararea a patru scenarii de simulare, corespunzătoare unor limite de viteză de 30 km/h și 50 km/h, cu și fără strategia de optimizare propusă. Rezultatele indică reduceri ale consumului de energie de aproximativ 16% la 30 km/h și peste 35% la 50 km/h, cu un impact limitat asupra timpului de parcurs. Concluziile demonstrează că optimizarea software a strategiilor de conducere poate îmbunătăți semnificativ eficiența energetică a vehiculelor autonome destinate transportului public urban, oferind o soluție viabilă pentru mobilitatea sustenabilă.*

Keywords: *Autonomous vehicle, Intelligent control system, Energy efficiency, Public transport, IPG CarMaker, Optimization*



Drd. ing.
Daniel-Levente NAGY
daniel.nagy@campus.utcluj.ro



Drd. ing.
Gabriel PRUNEAN



Drd. ing.
Dan-Ștefan ȘANDOR

Universitatea Tehnică din Cluj-Napoca,
Departamentul de Autovehicule Rutiere și Transporturi,
Bd. Muncii, Nr. 103-105, 400641 CLUJ-NAPOCA,
România

1. INTRODUCTION

The modern society is increasingly focused on reducing the carbon footprint across all industrial sectors, with road transport remaining a significant contributor to greenhouse gas emissions. While Electric Vehicles (EV) successfully eliminate tailpipe emissions, their overall environmental impact is intrinsically linked to the energy mix employed for charging. Consequently, optimizing the energy consumption of these vehicles becomes essential to reduce the load on power grids and, mitigate emissions from thermal power plants. Unlike human drivers, whose throttle and brake inputs are often subject to inconsistency and variability, autonomous vehicles leverage advanced sensor (RADAR, LiDAR, cameras) and Artificial Intelligence algorithms to control vehicle dynamics with superior precision. This high-level control capability unlocks novel opportunities for optimizing both route planning and travel times.

Urban transport efficiency can be substantially enhanced by prioritizing public transit over private vehicular use. Deploying a single autonomous bus to replace multiple private cars mitigates traffic congestion and lowers specific energy consumption per passenger. However, the widespread implementation of such systems faces significant hurdles regarding object perception, ethical decision-making, and, notably, the energy efficiency of the driving algorithms. This paper proposes optimizing the energy efficiency of an autonomous shuttle bus by implementing an intelligent control strategy. The objective is to demonstrate that rigorous management of tractive force, tailored to the specific dynamics of public transport, can substantially contribute to the sustainability of urban mobility.

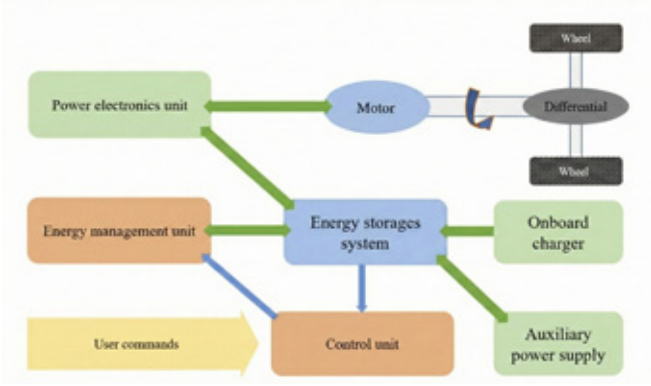


Figure 1. Electric vehicle architecture [7]

2. STATE OF THE ART

2.1. Electric Propulsion System Architecture

The design of an EV requires optimization of a complex system including the battery, power electronics, electric motor, and control system [12]. The typical architecture of an electric traction system (Figure 1) facilitates energy flow via electrical wires, thereby minimizing mechanical connections [8][14].

Power electronics regulate the energy flow between the storage system and the motor via DC/DC converters and DC/AC inverters [8][14]. The electric machine, exhibiting efficiencies ranging from 80% to 96%, is typically a Permanent Magnet Synchronous Motor (PMSM) or an Induction Motor (IM), capable of delivering high torque at standstill [14]. Regarding the transmission, the wide operational speed range of electric motors (up to 16,000 rpm) facilitates the use of a single-speed reduction gear, thereby eliminating the need for a conventional multi-speed gearbox [6][7]. Energy storage relies on electrochemical batteries or supercapacitors to handle peak power loads, as illustrated by the Ragone plot [8]. Recharging is performed using Alternating Current (AC) via the On-Board Charger (typically limited to ~20 kW) or Direct Current (DC) via high-power fast-charging stations (>250 kW) [4][20][21][22].

2.2. Automation Levels and Sensors

In accordance with SAE and NHTSA standards, driving automation is classified into a spectrum ranging from Level 0 (full human control) to Level 5 (full automation) [21]. AVs employ proprioceptive sensors (such as odometers and IMUs) to monitor internal vehicle dynamics, alongside exteroceptive sensors for environmental perception (Figure 2):

- RADAR and LiDAR: Facilitate obstacle detection and three-dimensional (3D) mapping.
- Video Cameras: Enable traffic sign recognition and road marking detection [1][3].

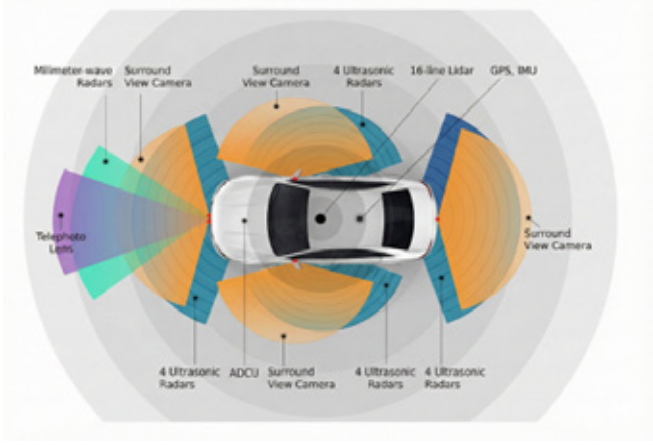


Figure 2. Sensor systems for autonomous vehicles [10]

2.3. Eco-Driving Algorithms and Artificial Intelligence (AI)

Eco-driving algorithms optimize energy consumption through precise acceleration control and deceleration anticipation [5][11][13]. The deployment of these strategies is supported by Vehicle-to-Everything (V2X) communication, which include interactions with infrastructure (V2I) and surrounding vehicles (V2V) [9][10].

Artificial Intelligence facilitates decision-making (driving policy) via Machine Learning techniques (Figure 3). These approaches encompass Supervised Learning (regression/classification), Unsupervised Learning (clustering), and Reinforcement Learning, employing Deep Neural Networks (Deep Learning) to replicate human-like decision-making processes within complex environments [9][18].

2.4. Comparative Analysis

Recent studies emphasize the critical role of simulation platforms in assessing the performance metrics of electric vehicles. For instance, Iclodean et al. [11] examined the deployment of autonomous shuttles in public

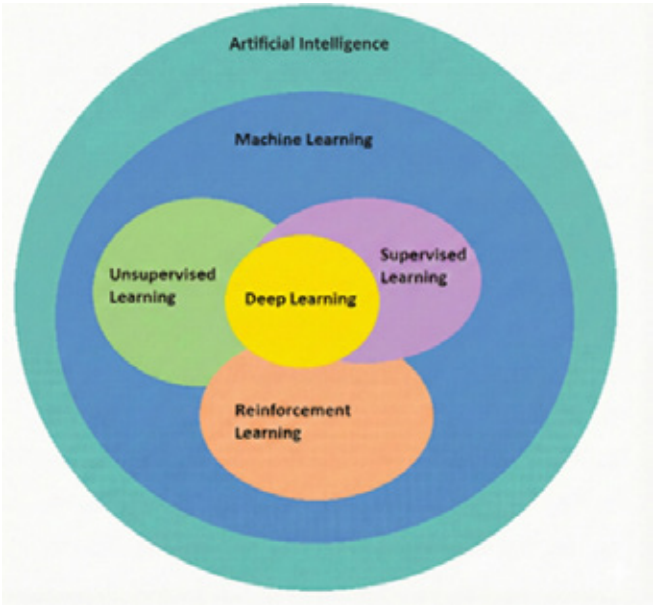


Figure 3. Artificial Intelligence and its subfields [18]

transportation, identifying the EasyMile EZ10 platform as a benchmark for conducting virtual testing scenarios. Within this framework, complex eco-driving strategies, such as those proposed by Ojeda [19] or Meng [15], can be adapted and simplified through coasting techniques. As demonstrated in the present study, this approach achieves significant energy consumption reduction without necessitating additional hardware implementation costs.

3. THEORETICAL APPROACH TO OPTIMIZATION

3.1. Optimization of the Energy Management System (EMS)

The energy efficiency of EVs can be significantly enhanced by regulating the power flow directed toward auxiliary systems, particularly the Heating, Ventilation, and Air Conditioning (HVAC) unit [1]. Previous research employed a MATLAB-Simulink model integrating a Fuzzy Logic controller (Figure 4) to manage battery consumption in a predictive manner, mimicking human reasoning [2][17].

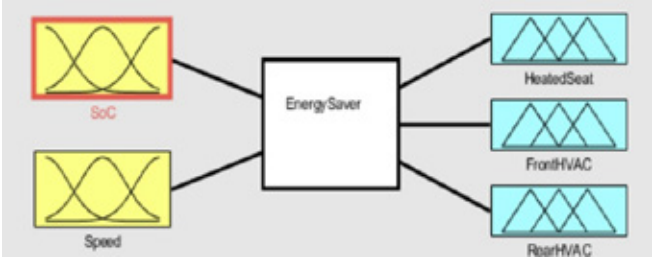


Figure 4. Fuzzy controller [2]

The battery state of charge (SoC) is determined by the relationship (1) [13]:

$$SoC = \frac{C_{max} - C_{used}}{C_{max}} \quad (1)$$

where C_{max} denotes the maximum capacity, and C_{used} represents the consumed capacity.

Simulations conducted on the NEDC and Japan 10-15 driving cycles demonstrated that implementing the Fuzzy Logic strategy facilitates a reduction in HVAC energy consumption with minimal impact on motor

torque. On the NEDC cycle, the operational autonomy was extended from 20,774 s (without management) to 25,013 s, representing a significant improvement in overall energy efficiency [2].

3.2. Algorithm Optimization for Autonomous Vehicles

Regarding trajectory optimization, current research focuses on the interaction between the Autonomous Vehicle (AV) and signalized infrastructure (V2I). The primary objective is to enable non-stop intersection crossing, thereby minimizing both energy consumption and travel time [15][16].

The mathematical model for optimizing speed (v) and acceleration (u) over the distance (l) relative to the traffic light incorporates safety constraints (β) and the dynamic braking distance (a). The optimization cost function (J) integrates travel time and passenger comfort:

$$J = \rho_t(t_p - t_0) + \rho_u \int_{t_0}^{t_p} u^2(t)dt \quad (2)$$

where (ρ_t) and (ρ_u) are weighting factors for time and energy consumption/comfort, respectively [15].

Results indicate that a weighting factor of $\rho < 0.7$ yields an optimal balance: travel time decreases by 42.84%, while energy consumption increases by only 4.85% relative to the baseline scenario, demonstrating the efficacy of predictive control within the urban environment (Figure 5) [15].

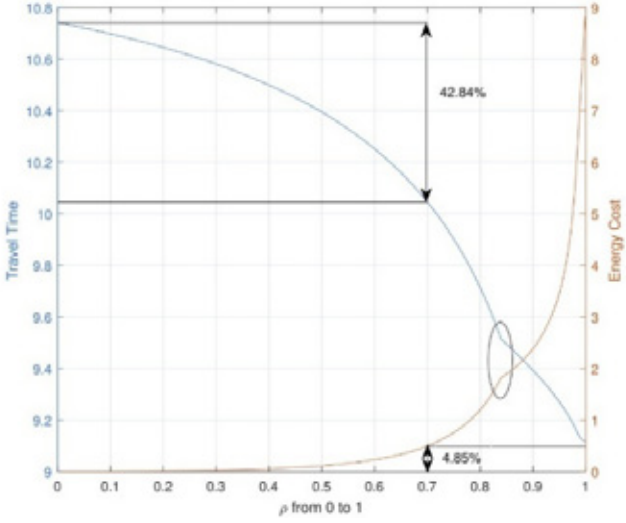


Figure 5. The trade-off between travel time and energy consumption [15]

4. SOFTWARE IMPLEMENTATION AND MODELING

To ensure the statistical relevance of the data, each test scenario was executed 10 consecutive times within the IPG CarMaker environment, utilizing an integration time step of 1 ms. A standard deviation in energy consumption of less than 0.02% was observed, confirming that the results are highly reproducible and unaffected by numerical solver errors. All simulations were conducted assuming a constant vehicle mass (excluding additional payload/passengers) to isolate the specific impact of the control algorithm.

4.1. Autonomous Vehicle Configuration

The IPG CarMaker platform, integrated with MATLAB-Simulink, was utilized for the simulation process. The selected vehicle is the EasyMile EZ10 autonomous shuttle (Figure 6), an electric vehicle optimized for urban public transportation. The kinematic and dynamic model of the vehicle was sourced from the pre-existing model library of the IPG CarMaker platform, as the research objective is focused exclusively on the optimization of the control algorithm. The parameters of this baseline model were subsequently calibrated to match the technical specifications of the EasyMile EZ10 (Table 1), utilizing a battery capacity of 30.72 kWh (LiFePO4) and a total mass of 2050 kg. Crucially, a constant vehicle mass corresponding to the curb weight (0% passenger load) was maintained across all simulation scenarios. This methodological choice was intended to isolate the specific impact of the proposed control algorithm on energy efficiency, eliminating the variable of fluctuating payload to ensure that the observed performance metrics are attributable solely to the software strategy. These specifications serve as the foundation for ensuring a high degree of realism within the IPG CarMaker simulation.



Figure 6. EasyMile EZ10 in the IPG CarMaker simulation environment

The propulsion system was adapted within the platform and defined as an asynchronous electric unit, directly coupled to a fixed-ratio transmission on the rear axle. The model incorporates motor efficiency maps, mechanical losses, and high-voltage battery characteristics. Sensors (LiDAR, RADAR, Cameras) were positioned according to real-world specifications via the *Sensor Mounting sub-menu*, enabling the vehicle to interact effectively with the virtual environment.

Table 1.
EasyMile EZ10 Technical Specifications

Parameter / System	Technical Details / Function
Dimensions (L x W x H)	4020 mm x 1998 mm x 2871 mm
Weight (Empty / Maximum)	2.050 kg / 3.050 kg
Propulsion / Battery	Asynchronous electric motor / LiFePO4 (30,72 kWh)
Performances	Max. speed 40 km/h; Autonomy up to 14 hours
Capacity	12 passengers (6 seated / 6 standing)
LIDAR sensors (2D/3D)	3D mapping, precision positioning and obstacle detection
RADAR sensors	Determining the distance to objects
Video cameras	Object recognition, traffic signs and traffic lights
GPS / IMU	Precision positioning (D-GPS) and inertial tracking
Odometry / CAN	Wheel speed and displacement measurement
Communications / V2X	4G connection for environmental surveillance and interaction

4.2. Road Infrastructure and Test Route

The simulated route reproduces a real-world sector in Cluj-Napoca: Piața Mărăști to Grădini Mănăștur (Figure 7). The map was generated by importing a KML file from Google Earth, incorporating the elevation profile to analyze the influence of road gradient (uphill/downhill) on energy consumption. The route comprises 8 stations, maintaining real-world distances and coordinates. An isolated 'dedicated bus lane' scenario was selected to precisely quantify the impact of the coasting strategy on energy efficiency, thereby eliminating statistical variables introduced by disruptive traffic. However, station stops were simulated as fixed events, compelling the software to calculate the optimal deceleration trajectory, this scenario can be expanded in future research by integrating traffic, pedestrians and cyclists as unforeseen braking factors.



Figure 7. Google Earth view of the selected road sector and the elevation profile of the road in CarMaker (in meters)

4.3. Control Strategy and Maneuver Optimization

The primary objective is to minimize energy consumption through intelligent control of the accelerator pedal. The proposed strategy replaces the conventional constant-speed maintenance up to the braking point with an optimized sequence. The vehicle accelerates to the reference speed, which it maintains in cruising mode until reaching a pre-calculated critical distance (x). At this optimal point, the accelerator pedal position signal is switched to value 0 (0% load), utilizing kinetic energy to traverse the remaining distance to the station exclusively via coasting.

Table 2 details the logical sequence of Maneuver list within CarMaker. A transition is observed from the acceleration and speed maintenance phase (*Maneuver 1)* to the calculation and coasting phase (Maneuver 2), where the accelerator pedal reference value is set to 0 (unactuated). This allows the resistive forces described in equations (3-6) to naturally decelerate the vehicle down to a threshold of 5 km/h near the stopping point. Maintaining this residual speed is essential to compensate for cumulative errors inherent in long-distance coasting (e.g., over 1 km).

Table 2.
IPG CarMaker Maneuver list

Step ID/ Order	Instruction
0	Wait 4s for initialisation
1	Speed up to 50km/h
2	Release gas pedal x meters before station
3	Speed up to 50km/h
4	Release gas pedal x meters before station
5	Speed up to 50km/h
6	Release gas pedal x meters before station
7	Speed up to 50km/h
8	Release gas pedal x meters before station
9	Speed up to 50km/h
10	Release gas pedal x meters before station
11	Speed up to 50km/h
12	Release gas pedal x meters before station
13	Speed up to 50km/h
14	Release gas pedal x meters before station

Consequently, at 5 km/h, the system regains control authority, enabling precise actuation of the braking system for fine positioning (with centimeter-level accuracy) exactly at the marked station point.

4.4. Mathematical model in MATLAB-Simulink

The real-time calculation of the optimal throttle release point is performed within Simulink (Figure 8), based on the cumulative effect of the following resistance forces:

Rolling resistance: F_{rr}: $F_{rr} = C_{rr} \cdot m \cdot g$ (3)

Aerodynamic drag: F_d: $F_d = \frac{1}{2} \cdot C_d \cdot \rho_{air} \cdot A_{frontal} \cdot v^2$ (4)

Gradient/Tilt resistance: F_{inc}: $F_{inc} = m \cdot g \cdot \sin(\theta)$ (5)

Where the parameters utilized in Equations (3-5) are defined as follows: $C_{rr}[-]$– rolling resistance coefficient (set to 0.012 according to tire specifications), $m[kg]$ – total vehicle mass (2050 $[kg]$), $[m/s^2]$ – gravitational acceleration (9,81 m/s^2), C_d [-] – aerodynamic drag coefficient (0.45 for the EasyMile profile), ρ_{air} $[kg/m^3]$– air density at 20°C (1,204 kg/m), A_{front}

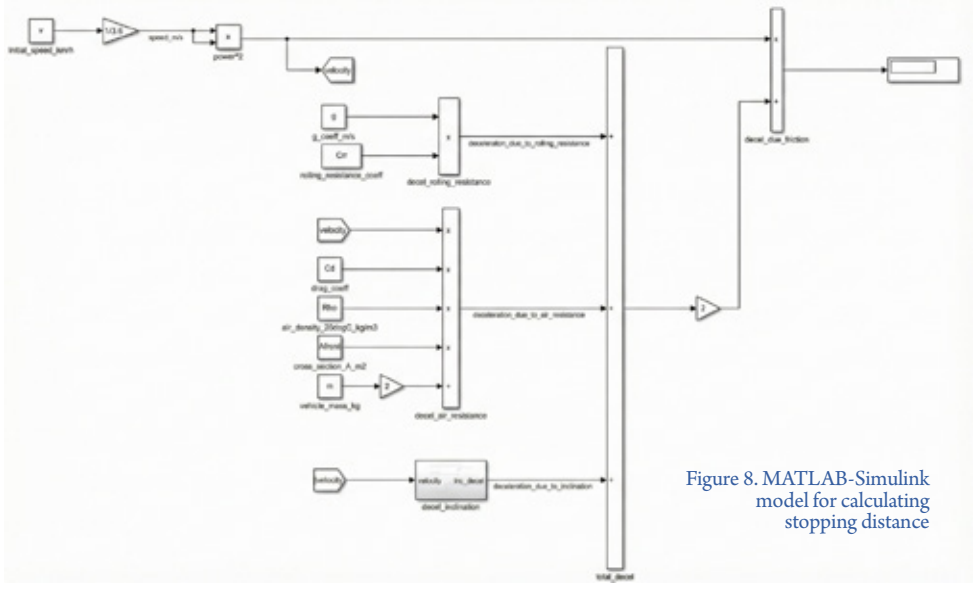


Figure 8. MATLAB-Simulink model for calculating stopping distance

$[m^2]$ – vehicle frontal cross-sectional area (4,8 m^2), v $[m/s]$– instantaneous vehicle speed, θ $[rad]$ – road inclination angle (extracted from the route's GPS profile), d_{stop} $[m]$ – estimated stopping distance in coasting mode.

The total deceleration (a_{total}) corresponds to the sum of the partial resistive decelerations calculated in equations (3-5). The estimated stopping distance (d_{stop}) is determined via the principle of energy conservation:

$$d_{stop} \approx \frac{\Delta v^2}{2 \cdot a_{total}} \quad (6)$$

The system commands the release of the accelerator pedal such that the vehicle reaches a residual speed of 3-5 km/h in the vicinity of the station. At this point, mechanical braking is applied to ensure precise positioning. This methodology eliminates energy consumption during the coasting phase and maximizes the overall efficiency of the propulsion system.

5. RESULTS AND DISCUSSION

Performance evaluation was conducted across four simulation scenarios (Table 3), contrasting the baseline cases (Default) against the optimized strategies (Optimised). The analysis focuses on two distinct speed thresholds: 30 km/h, representing the current operational limit for autonomous shuttles, and 50 km/h, corresponding to the standard urban speed limit.

Table 3.
Explanation of the four cases

Scenario	Max. speed	Coasting	Name in graphics
Case 1	30 km/h	NO (Default)	Case 1
Case 2	30 km/h	YES (Optimised)	Case 2
Case 3	50 km/h	NO (Default)	Case 3
Case 4	50 km/h	YES (Optimised)	Case 4

5.1. Energy Consumption Analysis (SoC)

The results indicate a significant reduction in energy consumption within the optimized scenarios. At a velocity of 30 km/h, the battery State of Charge (SoC) depletion over the 4099 m route decreased from 0.6010% (Case 1) to 0.5032% (Case 2), representing an energy saving of approximately 16%. In the 50 km/h scenario, the optimization strategy reduced consumption from 0.8974% to 0.5775%, yielding an improvement exceeding 35% (Table 4). Additionally, Figure 9 highlights the specific energy demand upon arrival at each station, allowing for a direct correlation between consumption rates and the road's elevation profile. Consequently, the variations in energy drop across different segments reflect the topological complexity and the variable load imposed by the route's gradient.

Table 4
Differences in battery charge state in each case

Distance [m]	Case 1	Case 2	Case 3	Case 4
0 (Start)	0.0000	0.0000	0.0000	0.0000
501.44	0.0641	0.0493	0.1043	0.0576
1171.92	0.1407	0.1123	0.2249	0.1336
2111.68	0.2487	0.1912	0.4115	0.2276
3273.55	0.4140	0.3278	0.6601	0.3867
4099.84 (Finish)	0.6010	0.5032	0.8974	0.5775

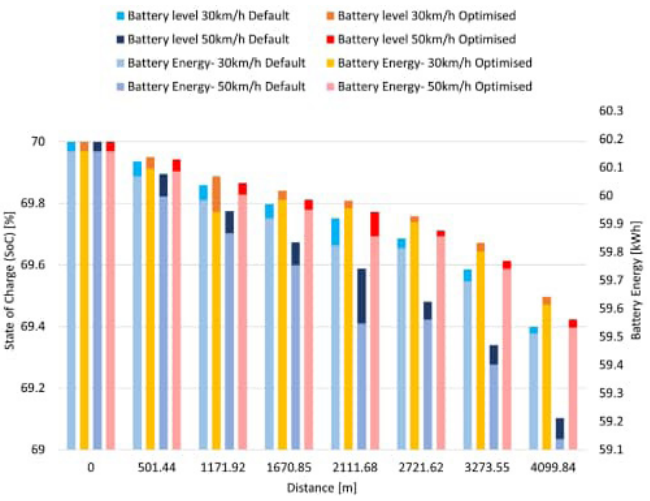


Figure 9. Distance over state of charge and battery energy in all four cases compared

5.2. Pedal Position and Control Strategy

The comparative analysis of acceleration and braking maps (Figure 10 vs. Figure 11) validates the efficacy of the proposed algorithm. In the 'Default' mode, the vehicle sustains acceleration until reaching the immediate proximity of the station, followed by abrupt braking (exhibiting brake pedal spikes of 40–60%). Conversely, in the 'Optimised' mode, the accelerator pedal is released anticipatively, allowing the vehicle to traverse the final segment via coasting. Consequently, the final braking application is minimal (below 10% load), required solely for precise stopping at speeds under 5 km/h.

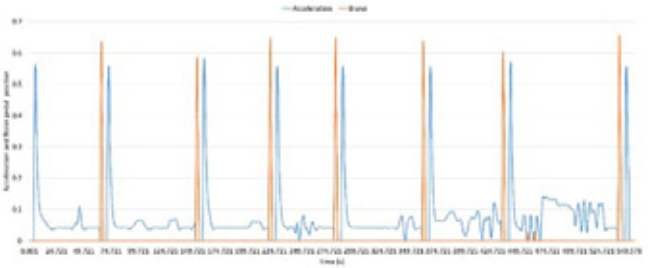


Figure 10. Time over acceleration and brake pedal position first case.

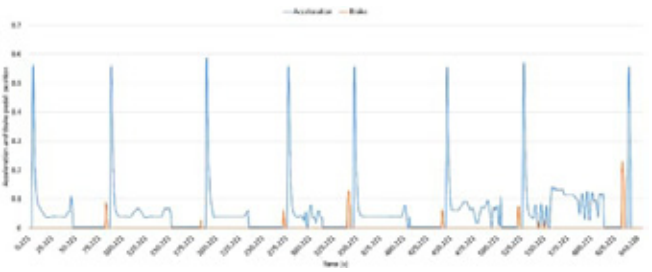


Figure 11. Time over acceleration and brake pedal position second case

5.3. Impact on Travel Time

While the implementation of the coasting strategy introduces a marginal time penalty, this trade-off is offset by substantial gains in energy efficiency. The energy consumption results obtained for the baseline scenario (Case 1) were cross-referenced with experimental data reported in the specialized literature for the EZ10 platform. Given that a 0.6% State of Charge (SoC) depletion over a distance of 4.1 km corresponds to a specific energy consumption of approximately 0.43–0.45 kWh/km, these

values align closely with performance metrics monitored in real-world urban tests (where consumption typically ranges between 0.4 and 0.5 kWh/km, depending on payload and climatic conditions). This correlation, of over 90%, validates the fidelity of the virtual model and the computational algorithm developed within Simulink.

Notably, Case 4 (50 km/h Optimised) presents the optimal trade-off: it exhibits lower energy consumption than the baseline Case 1 (30 km/h Default) while maintaining a nearly identical travel time (+1.16%, Table 5). This demonstrates that a higher operational speed, when combined with software optimization, constitutes an ideal solution for autonomous urban public transport.

Table 5.
Average time difference between cases

Test scenario	Time difference vs. Reference [%]
Case 1 (30 km/h Default)	0.00 (Reference)
Case 2 (30 km/h Optimised)	+ 22.79 %
Case 3 (50 km/h Default)	- 35.80 %
Case 4 (50 km/h Optimised)	+ 1.16 %

6. CONCLUSION AND PERSONAL CONTRIBUTIONS

6.1. Conclusion

This paper analyzed the potential for software-based optimization of the electric autonomous vehicle propulsion system, with a specific focus on urban public transport applications. By implementing an intelligent acceleration control strategy based on coasting, it was demonstrated that energy efficiency can be significantly enhanced without requiring modifications to the vehicle's hardware architecture.

Simulation results obtained within the integrated IPG CarMaker and MATLAB-Simulink environment indicate that, for the 30 km/h speed limit, energy consumption was reduced by approximately 16%, whereas for the 50 km/h limit, the reduction exceeded 35%. Although the coasting strategy introduces a moderate travel time penalty at lower speeds, the optimized 50 km/h scenario offers the optimal trade-off between energy efficiency and operational performance, exhibiting a travel time nearly identical to the baseline scenario yet with considerably lower energy consumption.

6.2. Personal Contributions

The primary contribution of this study lies in the development and validation of a control strategy directly applicable to autonomous driving systems, which leverages vehicle dynamics and environmental data to minimize energy losses. The proposed approach highlights the essential role of driving algorithm optimization in enhancing the sustainability of autonomous public transport.

6.3. Future Research Directions

Future research directions include extending the model to encompass complex traffic scenarios, integrating interactions with unfavorable signalized intersections, evaluating the influence of vehicle payload, and performing experimental validation under real-world operating conditions. These steps are crucial for consolidating the industrial applicability of the proposed strategy and for its implementation in large-scale urban transport systems.

REFERENCES:

[1] Abdullah, M., Faruque, A., Vatanparvar, K., „Modeling, Analysis, and Optimization of Electric Vehicle HVAC Systems", IEEE.
[2] Abulifa, A.A., Che Soh, A.B., Hassan, M.K., et al., „Energy Management System in Battery Electric Vehicle Based on Fuzzy Logic Control to Optimize the Energy Consumption in HVAC System", 2020.
[3] Ahmadi, M., Kiaei, P., Emamdoost, N., „SN4KE: Practical Mutation Testing at Binary Level", arXiv preprint, 2021.
[4] Chakraborty, S., Vu, H.N., et al., „DC-DC Converter Topologies for Electric Vehicles, Plug-in Hybrid Electric Vehicles and Fast Charging Stations: State of the Art and Future Trends", Energies, 2019.
[5] Chao-Yang, L., Yu-Ci, S., „Intelligent Eco-driving Guidance for Autonomous Driver System", Green Vehicle Development Division Automotive Research and Testing Center, Taiwan.
[6] Cîrmaci, M.V., Paraschiv, T., „Considerations regarding the energy efficiency of electric drive systems for special utility vehicles", Romanian Journal of Automotive Engineering (RoJAE), vol. 27, no. 2, 2021.
[7] El Hadraoui, H., Zegrari, M., Chebak, A., Laayati, O., Guennouni, N., „A Multi-Criteria Analysis and Trends of Electric Motors for Electric Vehicles", World Electr. Veh. J., 2022.
[8] Group, T.M., „Solving the Power/Energy Paradox for High-Power Defense Applications", Aerodefensetech, [Online]. Disponibil la: aerodefensetech.com.
[9] Grigore, L.S., „Architectures for autonomous vehicle control systems implemented in virtual simulation environments", Proceedings of the SIAR International Congress of Automotive and Transport Engineering, 2019.
[10] Henry Alexander Ignatious, Hesham-El-Sayed, Manzoor Khan, „An overview of sensors in Autonomous Vehicles", International Workshop on Smart Communication and Autonomous Driving (SCAD 2021) November 1-4, 2021, Leuven, Belgium.
[11] Iclodean, C., Cordoş, N., Varga, B.O., „Autonomous Shuttle Bus for Public Transportation: A Review", Technical University of Cluj-Napoca, 2020.
[12] Janiaud, N., Vallet, F.X., Petit, M., Sandou, G., „Electric vehicle powertrain simulation to optimize battery and vehicle performances", IEEE Vehicle Power and Propulsion Conference, 2010.
[13] Johnson, V., „Battery performance models in ADVISOR", J. Power Sources, 2002.
[14] Karki, A., Phuyal, S., Tuladhar, D., Basnet, S., Shrestha, B.P., „Status of Pure Electric Vehicle Power Train Technology and Future Prospects", Appl. Syst. Innov., 2020.
[15] Meng, X., Cassandras, C.G., „Eco-Driving of Autonomous Vehicles for Nonstop Crossing of Signalized Intersections", IEEE, 2020.
[16] Mitrea, M., „Computational simulation of dynamic stability for multi-axle vehicles under variable loading conditions", Romanian Journal of Automotive Engineering (RoJAE), vol. 26, no. 3, 2020.
[17] Milanes, V., Perez, J., Onieva, E., Gonzalez, C., „Controller for urban intersections based on wireless communications and fuzzy logic", IEEE Trans. Intell. Transp. Syst., 2010.
[18] Namatherdhala, B., Mazher, N., Sriram, G.K., „Uses Of Artificial Intelligence In Autonomous Driving And V2X Communication", International Research Journal of Modernization in Engineering Technology and Science, 2022.
[19] Ojeda, L.L., Han, J., Sciarretta, A., De Nunzio, G., Thibault, L., „A Real-time Eco-Driving Strategy for Automated Electric Vehicles", IEEE 56th Annual Conference on Decision and Control (CDC), 2017.
[20] Sujitha, N., Krithiga, S., „RES Based EV Battery Charging System: A Review", Renew. Sustain. Energy Rev., 2017.
[21] Van Brummelen, J., O'Brien, M., Gruyer, D., Najjaran, H., „Autonomous vehicle perception: The technology of today and tomorrow", Advanced Control and Intelligent Systems Laboratory, University of British Columbia, 2018.
[22] Vanholme, B., Gruyer, D., Lusetti, B., Glaser, S., Mammar, S., „Highly automated driving on highways based on legal safety", IEEE Transactions on Intelligent Transportation Systems, vol. 14, no. 1, pp. 333-347, March 2013.

NUMERICAL ANALYSIS OF TURBULENCE ENHANCING PISTON GEOMETRY IN A COMPRESSION IGNITION INTERNAL COMBUSTION ENGINE

ANALIZA NUMERICĂ A UNEI GEOMETRII A PISTONULUI DESTINATĂ INTENSIFICĂRII TURBULENȚEI ÎNTR-UN MOTOR CU ARDERE INTERNĂ CU APRINDERE PRIN COMPRIMARE

ABSTRACT: *The purpose of this study is to numerically analyze the influence of turbulence generating cavities arranged on the surface of a piston used in a research compression ignition internal combustion engine derived from the Cummins N14 heavy-duty engine series. The research is divided into three main sections that aim to study the influence of varying the diameter, depth and position of the turbulence generating cavities on the combustion performance indicators such as the thermal efficiency of the combustion cycle and the generated soot mass. The analyzed engine uses an 8-hole injector and the fuel composition defined in Ansys Forte 2024 R2 consists of n-heptane. The fuel injection starts at 22.5 [°] before TDC and the total injected mass per cycle is 0.0535 [g]. The results demonstrated that placing two concentric circles of turbulence generating cavities at the center of the piston cup, between the injector holes, with an angular spacing of 45 [°] and a diameter of 5.66 [mm], led to an increase in the thermal efficiency of the engine cycle of 1.61 [%] compared to the standard piston geometry.*

REZUMAT: *Scopul prezentului studiu constă în analiza numerică a influenței cavităților generatoare de turbulență dispuse pe suprafața unui piston utilizat într-un motor cu ardere internă cu aprindere prin comprimare, destinat cercetării și derivat din seria de motoare pentru aplicații grele, Cummins N14. Lucrarea este divizată în trei secțiuni principale care urmăresc studierea influenței pe care modificarea diametrului, adâncimii și a poziționării cavităților generatoare de turbulență o exercită asupra indicatorilor performanței de ardere, precum eficiența termică a ciclului de ardere și masa de carbon generată în urma procesului de ardere. Motorul analizat utilizează un injector cu 8 orificii iar compoziția combustibilului definit în Ansys Forte 2024 R2 constă în n-Heptan. Injecția de combustibil este realizată cu un avans de 22.5 [oRAC] față de punctul mort interior, iar masa totală de combustibil injectată pe ciclu este de 0.0535 [g]. Rezultatele obținute demonstrează faptul că, plasarea cavităților generatoare de turbulență în regiunea centrală a cupei pistonului conform unui tipar definit de două cercuri concentrice și având fiecare cavitate dispusă la jumătatea lungimii arcului de cerc definit de două orificii consecutive ale injectorului, cu un increment de 45 [oRAC] și un diametru al cavităților de 5.66 [mm], a condus la o creștere de 1.61 [%] a eficienței termice globale a ciclului motor, comparativ cu geometria standard a pistonului.*

Keywords: *Keywords: CFD, diesel, injection, turbulence, combustion chamber, piston bowl*



Drd. ing.
Andreeas Marco FÁRCAȘ [2)]
andreeas.farcas@student.upt.ro



Prof. dr. ing.
Dorin LELEA [1)]

1) Universitatea Politehnica din Timișoara, B-dul Mihai Viteazu, Nr. 1, 300222 TIMIȘOARA, România
2) Continental Automotive Romania, Str. Siemens, Nr. 1, 300704 TIMIȘOARA, România

NOMENCLATURE

cp: specific heat, J/kg·K
δ: Kronecker Delta, -
k: thermal conductivity, W/m·K
p: pressure, Pa
P: mean pressure, Pa
ρ: density, kg/m^3
t: time, s
T: temperature, K
u: velocity, m/s
U: mean velocity, m/s
μ: dynamic viscosity, Pa·s
x, y, z: coordinate, m
ATDC: after top dead center, -
CA: crank angle, -
CFD: computer fluid dynamics, -
TDC: top dead center, -

1. INTRODUCTION

Increasingly stringent environmental regulations are forcing the automotive industry companies to shift their knowledge and strategies towards electrification and hybridization technologies. According to European Parliament representatives [12], by 2050 the carbon footprint generated by internal combustion engines used in personal transportation will be completely neutralized. On the other hand, heavy industries like long-haul freight transportation, mining, maritime and mobile power generation cannot rely solely on electric propulsion systems and so, these industries are now dealing with the pressure of developing more sustainable and future-proof propulsion systems at a faster than ever before pace.

1.1. Scientifical background

Wu A. et al conducted a CFD optimization of a stepped lip dimpled piston geometry in a medium duty diesel engine [10]. The CFD improved turbulence generating piston geometry was experimentally analyzed at Sandia Off-Road Diesel Research Engine Facility and the results obtained for early injection timings showed a 45 [%] decrease in soot mass, a 20 [%] reduction in CO mass, and a thermal efficiency increase of 0.5 [%].

Brusiani F. et al investigated, by means of numerical simulation, the correlation between the injector hole geometry and the spray characteristics for a common rail diesel engine [2]. Three types of injector hole geometries were investigated: cylindrical hole, k hole and ks hole. The ks hole geometry demonstrated the best results from a flowing stability standpoint. Furthermore, the rounded edge at the entrance section of the ks hole guaranteed that the vapor generation risk and thus, the risk of cavitation, was suppressed on the entire injector hole length.

Wang Z. et al studied the dynamics of internal flow and spray primary breakup mechanism in a common rail diesel injector using a split injection strategy [9]. It was discovered that cavitation is induced by two effects, namely the throttling effect which occurs at the needle seat and the flow redirection which occurs at the nozzle inlet. It was observed that the throttling induced cavitation occurs during the initial and final stages of the injection process at the needle seat region, when sudden drops of pressure appear, while the flow redirection occurs during the continuous, steady stage of the injection, where the local pressure is high.

Pos R. et al conducted an experimental study which emphasized the impact that the injector operating life has on the injector's spatial-time spray

evolution in the early stages of the injection process [8]. The analyzed injectors had the same part number and were divided into four groups depending on their operating life, which varied from new, never used before injectors, to injectors taken from an engine that ran up to 90000 miles. The experimental results showed that used injectors had a tendency of generating asymmetric spray penetration in the early stages of the injection due to hole-to-hole variations that occur because of carbonaceous deposits.

Huang W. et al studied the effects generated by the number of holes in multihole diesel injector nozzles on the spray dynamics by using the X-ray Phase-Contrast Imaging technique [6]. Five injector nozzle configurations were tested ranging from three to nine holes. The main finding in this study was a non-linear behavior of the spray dynamics for three, five and six-hole nozzles, whereas for the eight-hole injector nozzle the spray had a stable and predictable behavior. It was found out that further increasing the number of holes in the injector nozzle above eight led to the reoccurrence of the unstable spray dynamics.

Chen Z. et al conducted an experimental study on the effect of nozzle geometry on string cavitation using optical diesel nozzles, a high-speed Fastcam SA-Z CMOS camera, and a Questar QM-1 long distance microscope [5]. It was discovered that string cavitation is the main responsible factor for increased spray cone angle which is known to affect the initial combustion phase. Furthermore, smaller L/D0 ratios tend to encourage string cavitation more in the nozzle region than in the nozzle sac.

Busch S. et al studied the impact of a stepped-lip piston bowl and a conventional piston bowl on the thermal efficiency of a single cylinder research engine [3]. Out of the two, the stepped-lip piston bowl offered the best thermal efficiency improvements regardless of the injection timing, although the best results were obtained for the main injection timing starting between (3…13) [°] ATDC.

In another research, Busch et al analyzed, by means of CFD simulation, the bowl geometry effects on the turbulent flow structure in a direct injection diesel engine [4]. In this research, the appearance of recirculation volumes above the piston, induced by the dimpled piston geometry, explains the decreases in soot and carbon monoxide masses obtained in other experiments.

Zha K. et al conducted, by means of combustion image velocimetry, an experimental study regarding the effects of piston geometry on late-stage combustion in a light-duty research diesel engine [11]. The analyzed piston geometries were the re-entrant and stepped-lip piston bowl configuration. The main finding that can be depicted from this study consists in the existence of a vertical toroidal vortex in the proximity of the stepped-lip piston crown, around 50 [°] CA, which supposedly justifies the enhanced thermal performance of this configuration.

Kogo T. et al investigated, by means of numerical simulation, new ways of increasing the thermal efficiency of a Toyota Inline 4-Cylinder 2.8-liter ESTEC 1GD-FTV engine. It was demonstrated that using a taper lip combustion chamber improved the air-fuel mixing process to the point where the engine used 15 [%] less fuel in NEDC than the standard engine, while also achieving a maximum thermal efficiency of approximately 44 [%].

The present research proposes a solution to intensify the air-fuel interaction by enhancing in-cylinder turbulence to a level that allows a balanced air-fuel mixture creation throughout the entire volume of the combustion chamber, while, at the same time, mitigating the effects of unwanted phenomena like in-nozzle cavitation, which can affect the spray pattern and lead to the formation of rich fuel zones that are responsible for uncomplete burning. This solution consists of turbulence-generating cavities placed on the active surface of the piston. The number of turbulence generating cavities, as well as their diameter, depth, and positioning relative to the cylinder axis are chosen so that right after the injection starts, the air movement inside the combustion chamber helps with creating the conditions for a smooth burning initiation phase and that over the entire course of the burning process, the fluid mixture inside the cylinder creates favorable condition for prolonged unburned chemical species oxidation.

2. SIMULATION SETUP

2.1 Numerical simulation setup

The simulation software used for conducting this research is Ansys Forte 2024 R2, a state-of-the-art internal combustion engine simulation software that incorporates a chemical kinetics solver known as Chemkin [1]. One of the key features of this software, which is the AMG (Automatic Mesh Generation) was used for the discretization of the fluid volume contained in the combustion chamber when the piston is at TDC. The simulated geometry is represented by the combustion chamber of a single cylinder research engine used in Heavy-Duty Diesel and Gaseous-Fueled Engine Laboratory from Sandia National Laboratories. The analyzed combustion chamber is derived from the Cummins N-14 engine family and it's a slightly modified version fitted for optical research. The main modification is given by the cylindrical shape of the piston bowl which serves as an optic characteristic for combustion visualization. The key engine characteristics can be found in Table 1.

Table 1.
Analyzed engine key characteristics

Cr. No.	Parameter name	Value/Type
1	Bore x stroke [mm]	139.7 x 152.4
2	Piston bowl dimensions (width, depth) [mm]	97.9, 15.5
3	Displacement [cm3]	2340
4	Connecting rod length [mm]	304.8
5	Fuel injector type [-]	Common-Rail, pilot valve actuated
6	No. of injector holes [-]	8, equally spaced
7	Spray pattern included angle [°]	152
8	Nozzle orifice diameter [mm]	0.196
9	Nozzle orifice L/D [-]	0.5

The chemical composition of the fuel was defined using a pre-defined mixture data set for standard Diesel fuel provided by Ansys. For the spray proprieties, the Radius of Influence Model was used as the Droplet Collision Model and the Radius of Influence was set to 20 [mm]. The Vaporization Model was also accounted for. The inflow droplet temperature was set to 368 [K] and pulsed injection was chosen as the injection type. A discharge coefficient of 0.7 and a spray cone angle of 15 [°] were considered. The primary and secondary jet breakups were modeled by parametrizing the Kelvin-Helmholz, and the Rayleigh-Taylor model. The size constant of KH breakup and the time constant of RT breakup were kept to 1.0, while the time constant of KH breakup was considered to be 40 and the size constant of RT breakup, 0.15. The nozzle location was set using a cylindrical coordinate system, while the spray direction was set using a spherical coordinate system. The injector nozzle sits at 1.58 [mm]

inside the combustion chamber relative to the cylinder head and the spray is expelled from the nozzle at an angle of 104 [°] relative to the cylinder axis. The ignition start moment is 22.5 [°] ATDC and the duration of injection is 7.75 [°] CA. The injection profile was defined to be identical to the one used in the series engine. Besides the standard conservation of mass, momentum and energy equations, Ansys Forte uses the Reynolds-Averaged Navier Stokes equation to model the turbulent, in-cylinder flows. In the definition of the in-cylinder gaseous mixture, the residual gases were accounted for by considering the oxygen participation to be 12.6 [%] and the nitrogen participation to be 87.4 [%].

The conservation of mass:

$$\frac{\partial(\rho \cdot u_i)}{\partial x_i} = 0 \quad (1)$$

The conservation of momentum:

$$\frac{\partial(u_i \cdot \rho \cdot u_j)}{\partial x_i} = -\frac{\partial p}{\partial x_j} + \frac{\partial}{\partial x_i}\left(\mu \cdot \frac{\partial u_j}{\partial x_i}\right) \quad (2)$$

The conservation of energy:

$$\frac{\partial(\rho \cdot c_p \cdot u_i \cdot T)}{\partial x_i} = \frac{\partial}{\partial x_i}\left(k \cdot \frac{\partial T}{\partial x_i}\right) \quad (3)$$

The Reynolds averaged Navier Stokes partial differential equation in tensor form statistically describes the fluid particle motion within the flow:

$$\frac{\partial(\rho U_i)}{\partial t} + \frac{\partial(\rho U_i U_j)}{\partial x_j} = -\frac{\partial P}{\partial x_i} + \frac{\partial}{\partial x_j}\left[\mu\left(\frac{\partial U_i}{\partial x_j} + \frac{\partial U_j}{\partial x_i}\right) - \rho\overline{u_i' u_j'}\right] \quad (4)$$

Reynolds stress term resulted from the averaging process is given by the Boussinesq hypothesis:

$$-\rho\overline{u_i' u_j'} = \mu_t\left(\frac{\partial U_i}{\partial x_j} + \frac{\partial U_j}{\partial x_i} - \frac{2}{3}\frac{\partial U_k}{\partial x_k}\delta_{ij}\right) - \frac{2}{3}\rho k \delta_{ij} \quad (5)$$

The convergence criterion is defined as follows:

$$R^{\phi} = \frac{\sum_{cells,P}|\sum_{nb} a_{nb} \cdot \phi_{nb} + b - a_p \phi_p|}{\sum_{cells,P}|a_p \phi_p|} \quad (6)$$

3. RESULTS

3.1. Standard geometry results

Results for the standard geometric piston configurations are provided so that they will serve as a comparison base for all the following geometric configurations that use turbulence enhancing cavities.

Figure 1 illustrates a view from above of the research-adapted Cummins N14 piston geometry.

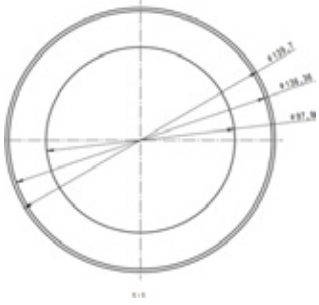


Figure 1. Standard piston geometry (view from above).

One of the most important aspects of quantifying the performance of the in-cylinder air-fuel mixture is represented by the visual analysis of the velocity magnitude plot, represented in Figure 2. a. To have a complete picture for all the combustion phases, a number of three plots were extracted for each simulation case, at 0 [°] ATDC, 45 [°] ATDC, and 65 [°] ADTC. One of the most important aspects visible in Figure 2. a. is the fact that, although the piston is at TDC, where all the fluid movement within the cylinder is mainly inertial driven, a high velocity magnitude can be observed in the vertical region of the piston bowl. This offers the benefit of avoiding the contact between cold drops of fuel and the hot vertical walls of the cup, which otherwise can represent another soot formation source. This phenomenon is also visible in figure 2. b., where it can be observed that soot-rich volumes are not forming in the combustion chamber walls proximity.

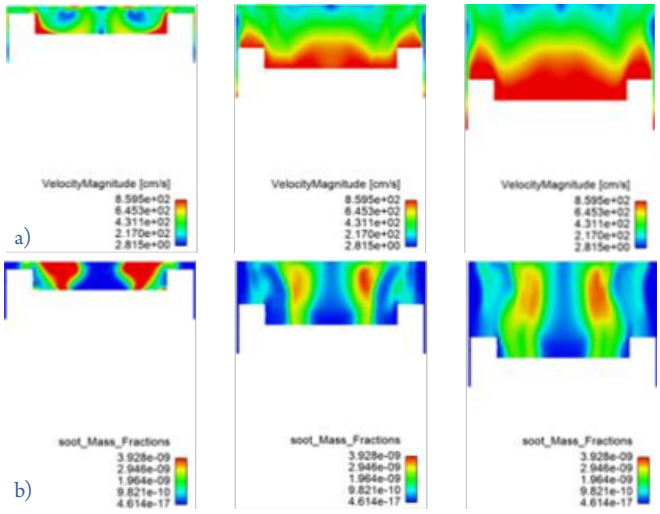


Figure 2. Standard piston geometry combustion plots.
a) Velocity magnitude plots. b) Soot mass fractions plot.

3.2 The influence of turbulence enhancing cavities diameter on the combustion process.

In this first analysis of turbulence enhancing cavities geometry influence, two study cases were considered. In Figure 3. a., the sphere that was used to generate the cavities has an 8 [mm] diameter, while the sphere used to generate the turbulence enhancing cavities captured in Figure 3. b. has a 9 [mm] diameter. In both cases the depth of turbulence generating cavities is 1 [mm].

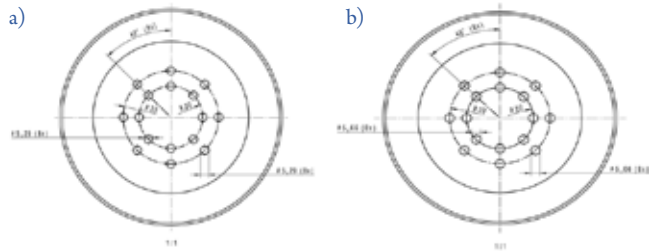


Figure 3. Case study no. 1 piston geometric configurations (view from above).
a) 8 [mm] diameter generating sphere. b). 9 [mm] diameter generating sphere.

In both cases studied, in the velocity magnitude plots represented in Figure 4. a. and Figure 5. a. it was observed that turbulence enhancing cavities promote the formation of multiple pressure micro-gradients. Those micro-gradients improve the oxidation process, especially in the central region of the piston cup, where most of the rich fuel pockets tend to develop.

In Figure 4. b. and figure 5. b., the reduced volume of soot is attributed to a prolonged oxidation phase that is sustained by the presence of turbulence enhancing cavities.

The correlation between the increased high velocity magnitude volume within the combustion chamber during the late burn stages, and the decreased soot formation volume, confirms the positive effect induced by

placing turbulence enhancing cavities in the central region of the piston cup, as illustrated in figures 4. a. and 5. a.

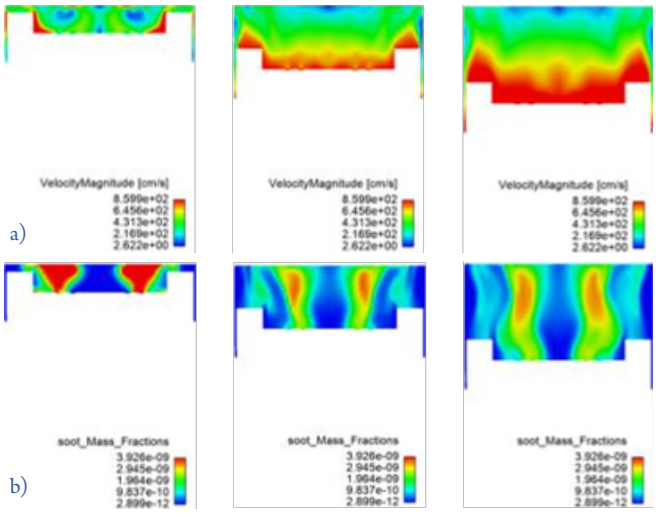


Figure 4. Case study no. 1. a. combustion plots.
a) Velocity magnitude plots. b) Soot mass fractions plots.

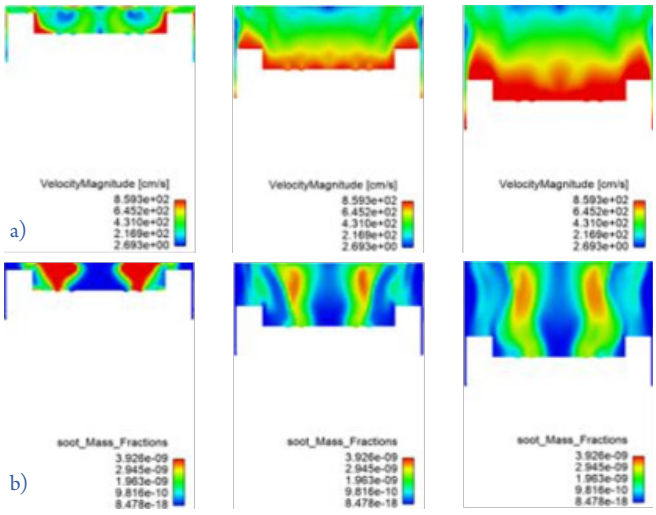


Figure 5. Case study no. 1. b. combustion plots.
a) Velocity magnitude plots. b) Soot mass fractions plots.

3.3 The influence of turbulence enhancing cavities depth on the combustion process.

The second case study performed in this research consists of two cases which differ from each other by the depth of the turbulence generating cavities. In the geometric configuration, visible in figure 6., the constant diameter sphere was used to generate turbulence enhancing cavities that are characterized by different depths, the turbulence enhancing cavities pictured in figure 6. a. having a depth of 1 [mm], and the turbulence enhancing cavities pictured in figure 6. b. having a depth of 1.5 [mm]. One particularity of this case study is that, besides varying the depth of the cavities, their positioning relative to the cylinder axis is modified to the periphery of the piston bowl. This was made to avoid unwanted effects such as premature spray disintegration due to highly intensified turbulent flows in the central region of the piston bowl and in the nozzle proximity. As can be seen in the velocity magnitude plots illustrated in figure 7. a., the studied configurations generate a distortion at the border that separates the high intensity velocity magnitude from the moderate intensity

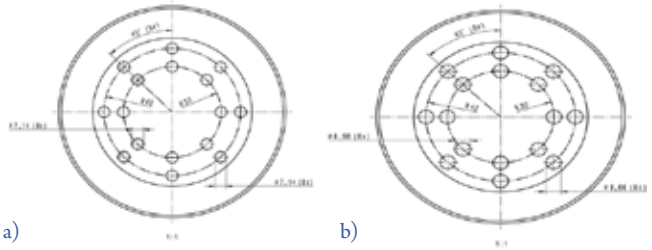


Figure 6. Case study no. 2 piston geometric configurations (view from above).
a) 1 [mm] deep cavities. b).1.5 [mm] deep cavities.

velocity magnitude. In figure 7. b., it can be observed that, at 0 [°] CA, pockets of soot form in the outer turbulence enhancing circle of cavities. This accumulation serves as an explanation for the 1.09 [%] increase in the remanent soot mass by comparison with the standard case, that is mainly attributed to the fact that, in those isolated regions of the combustion chamber, the diffusive burning conditions are hard to achieve as a consequence of rich fuel pockets, and thus, the soot mass present in those volumes cannot be further oxidized in the late combustion stages.

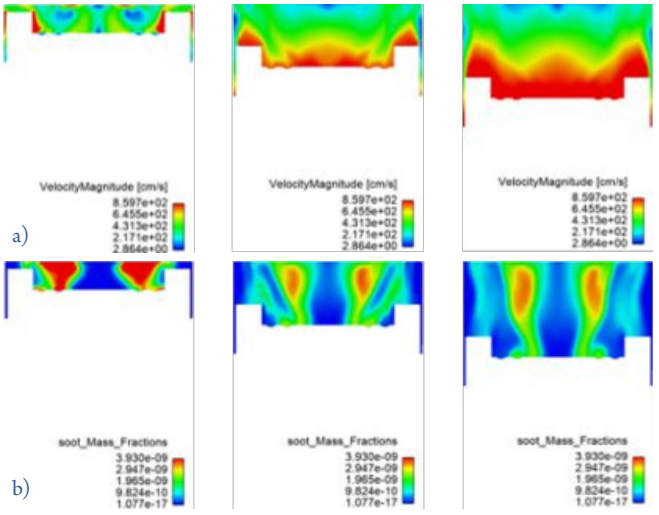


Figure 7. Case study no. 2. a. combustion plots.
a) Velocity magnitude plots. b) Soot mass fractions plots.

The 12.47 [%] decrease in the maximum soot mass generated during the combustion cycle can be identified in figure 7. b., where at 45 [°] ATDC, and at 65 [°] ATDC, the turbulence enhancing cavities through their aspiration effect that they create, are repositioning the soot masses in the central region of the combustion chamber, where highly turbulent flows are creating favorable conditions for further oxidation.

For the second case study in this depth analysis configuration, the higher depth of the turbulence enhancing cavities leads to a highly turbulent disruptive separation layer in the velocity magnitude that can be observed in figure 8. a. Consequently, a flow is generated in the outer zone of the piston bowl that segregates the soot mass fractions to the point where some of them are trapped in the circular flows near the cylinder walls. This phenomenon, visible in figure 8. b., leads to a 2.53 [%] increase in the stabilized soot mass, compared to the standard case.

3.4 The influence of turbulence enhancing cavities positioning on the combustion process.

Based on the results obtained in the previous configurations, a study on the influence of the turbulence enhancing cavities positioning relative to the cylinder axis was conducted. Considering that placing turbulence

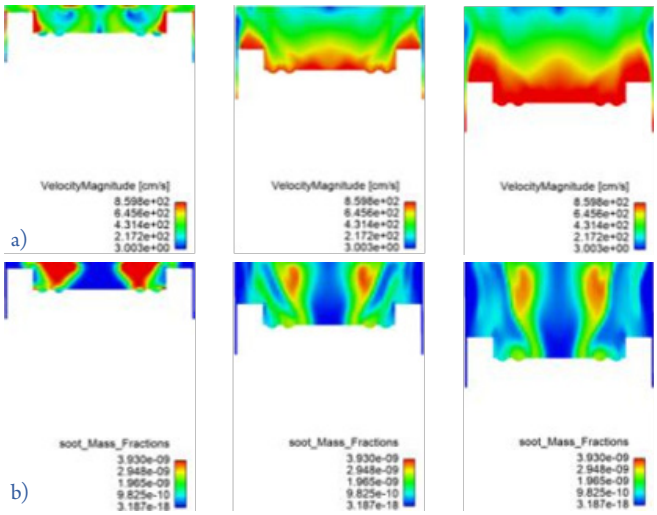


Figure 8. Case study no. 2. b. combustion plots.
a) Velocity magnitude plots. b) Soot mass fractions plots.

enhancing cavities in the central region of the piston bowl showed mixed results, depending on their positioning relative to the piston bowl walls, this configuration also analyses the effects generated by placing turbulence enhancing cavities in the proximity of the cylinder wall, like the one pictured in figures 9. a. and 9. b.

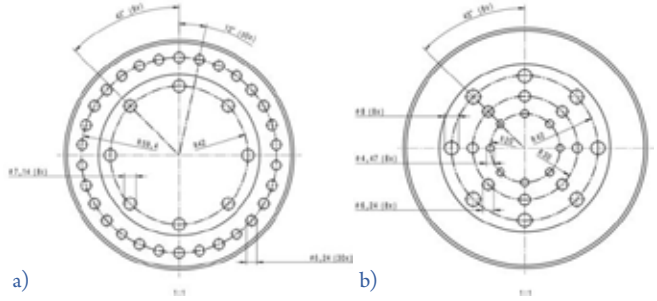


Figure 9. Case study no. 3 piston geometric configurations (view from above).
a) two outer circles of cavities. b) three inner circles of cavities.

For the first study case from this configuration, pictured in figure 9. a., the velocity magnitude plots, visible in figure 10. a., show a highly intensified velocity field in the interstice between the piston wall and the cylinder wall. This can be seen as a negative aspect due to increased wall heat losses, just as the pockets of soot rich zones which are present at TDC can, based on which it can be confirmed that placing turbulence enhancing cavities in the proximity of the piston bowl wall is not rational. The visible soot mass fractions volume reduction compared to the standard piston geometry, visible in figure 10. b. can be attributed to the highly turbulent movement generated by placing two rows of turbulence enhancing cavities in a region of piston bowl where the flow is already characterized by pronounced inertial effects.

One of the most visible changes in the velocity magnitude, illustrated in figure 11. a., and soot mass fraction evolution, visible in figure 11. b., is the one obtained for three circles of turbulence enhancing cavities placed in the central region of the piston bowl. This strengthens the conclusions of the first studied configurations, where it was observed that placing the cavities in the central region of the piston bowl generated the highest thermal efficiency increase in all the configurations studied.

4. CONCLUSIONS

Based on the three study cases performed, it can be concluded that placing turbulence enhancing cavities on the surface of a compression ignition internal combustion engine piston can lead to thermal efficiency increases together with soot mass and carbon monoxide reductions, but not in any configuration.

The improvements in thermal efficiency are largely impacted by the positioning of the turbulence enhancing cavities relative to the cylinder axis. In the first case study, the configuration with the largest diameter out of the two studied, with the placement of turbulence enhancing cavities in the central region of the piston, on two concentric circles, led to a thermal efficiency increase of 1.61 [%], together with an increase of 7.83 [%] for the stabilized soot mass.

The second analyzed case study, which studied the influence of turbulence enhancing cavities depth on the combustion process, demonstrated the fact that using two concentric circles of turbulence enhancing cavities in the central region of the piston bowl that use the lowest depth out of the two analyzed configurations managed to generate the third highest reduction in soot mass out of all the seven studied configurations.

The third case study, which analyzed the influence of the turbulence enhancing cavities positioning on the piston surface demonstrated the fact that placing the turbulence enhancing cavities in the cylinder wall proximity affects the oxidation process to the point where remanent carbon monoxide mass reaches the highest value of all the analyzed configurations.

REFERENCES:
[1] – Ansys Forte User Guide, ANSYS, Inc., Southpointe, 2600 Ansys Drive. Canonsburg, PA 15317.
[2] – Brusiani, F.; Falfari, S.; Pelloni, P., Influence of Diesel injector hole geometry on the flow conditions emerging from the nozzle. 68th Conference of the Italian Thermal Machines Engineering Association. ATI2013. Energy Procedia. Vol. 45, pp. 749 – pp. 758, 2014.
[3] – Busch, S.; Zha, K.; Kurtz, E.; Warey, A.; Peterson, R., Experimental and Numerical Studies of Bowl Geometry Impacts on Thermal Efficiency in a Light-Duty Diesel Engine. SAE Technical Paper. 2018-01-0228, 2018.
[4] – Busch, S.; Zha, K.; Perini, F.; Reitz, R.; Kurtz, E.; Warey, A.; Peterson, R., Bowl Geometry Effects on Turbulent Flow Structure in a Direct Injection Diesel Engine. SAE Technical Paper. 2018-01-1794, 2018.
[5] – Chen, Z.; He, Z.; Shang, W.; Duan, L.; Zhou, H.; Guo, G.; Guan, W., Experimental study on the effect of nozzle geometry on string cavitation in real-size optical diesel nozzles and spray characteristics. Fuel. Vol. 232, pp. 562 – pp. 571, 2018.
[6] – Huang, W.; Moon, S.; Gao, Y.; Wang, J.; Ozawa, D.; Matsumoto, A., Hole Number Effect on Spray Dynamics of Multi-Hole Diesel Nozzles: An Observation from Three to Nine-Hole Nozzles. Experimental Thermal and Fluid Science. ETF 9687, 2018.
[7] – Kogo, T., Hamamura, Y., Nakatani, K., Toda, T.; Kawaguchi, A.; Shoji, A., High Efficiency Diesel Engine with Low Heat Loss Combustion Concept - Toyota's Inline 4-Cylinder 2.8-Liter ESTEC 1GD-FTV Engine. SAE Technical Paper. 2016-01-0658, 2016.
[8] – Pos, R.; Wardle, R.; Cracknell, R.; Ganippa, L., Spatio-temporal evolution of diesel sprays at the early start of injection. Applied Energy. Vol. 205, pp. 391 – pp. 398, 2017.
[9] – Wang, Z.; Dai, X.; Li, F.; Li, Y.; Lee, C.-F.; Wu, H.; Li, Z., Nozzle internal flow and spray primary breakup closely coupled split injection strategy. Fuel. Vol. 228, pp. 187 – pp. 196, 2018.
[10] – Wu, A.; Cho, S.; Lopez Pintor, D.; Busch, S.; Federico, P.; Reitz, R. D., Effect of a CFD-improved dimple stepped-lip piston on thermal efficiency and emissions in a medium-duty diesel engine. International Journal of Engine Research. Vol. 24, Issue 5, pp. 2223 – pp. 2232, 2023.
[11] – Zha, K.; Busch, S.; Warey, A.; Peterson, R.C.; Kurtz, E., A Study of Piston Geometry Effects on Late-Stage Combustion in a Light-Duty Optical Diesel Engine Using Combustion Image Velocimetry. SAE Technical Paper. 2018-01-0230, 2018.
[12] – **https://www.europarl.europa.eu/topics/en/article/20221019STO44572/eu-ban-on-sale-of-new-petrol-and-diesel-cars-from-2035-explained, last accessed: 26.11.2025.

The EIGHTH EDITION OF THE SIAR SUMMER UNIVERSITY IN AUTOMOTIVE ENGINEERING
A OPTA EDIȚIE A UNIVERSITĂȚII DE VARĂ SIAR ÎN INGINERIA AUTOVEHICULELOR
UNIVIA 2026









În perioada 22–24 iulie 2026, studenții anului 4 de studiu de la specializarea Blindate, Automobile și Tractoare din cadrul Academiei Tehnice Militare ”Ferdinand I” au participat cu succes la cea de-a VIII-a ediție a Școlii de Vară UNIvIA 2026.

Evenimentul s-a desfășurat în colaborare cu Registrul Auto Român (RAR) și Societatea Inginerilor de Automobile din România (SIAR), oferind viitorilor ingineri o perspectivă practică și aplicată asupra cadrului legislativ și tehnic din industria de autovehicule și militară.

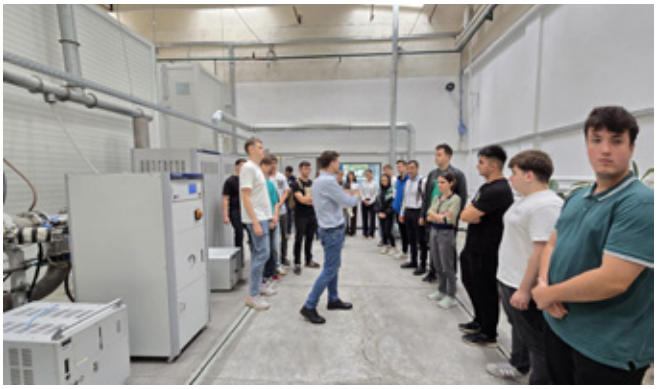
Școala de vară a debutat la sediul RAR din Voluntari unde studenții au luat parte la o serie de expuneri de specialitate susținute de experții instituției, precum și de cadrele didactice participante din Academia Tehnică Militară ”Ferdinand I”:

- Rolul RAR în domeniul reglementării, încercării/testării și certificării poluării autovehiculelor.
- Cadrul general de reglementare privind omologarea vehiculelor.
- Prezentarea RNTR 7 – Reglementările privind omologarea individuală, eliberarea cărții de identitate și certificarea autenticității vehiculelor rutiere.
- Aplicarea Regulamentului UE 2018/858 privind omologarea și supravegherea pieței autovehiculelor și remorcilor acestora, precum și ale sistemelor, componentelor și unităților tehnice separate.
- Prevederile Ordinului comun MTI-MApN nr. 1.224/M.219 privind omologarea națională a vehiculelor rutiere concepute, fabricate sau modificate pentru a fi utilizate exclusiv de forțele armate.

Componenta teoretică a fost completată de activități practice de mare interes:

- Analiza unui autovehicul militar românesc: Studenții au analizat cerințele și pașii necesari parcurgerii procesului de omologare pentru un vehicul militar de producție națională aflat în incinta RAR.
- Vizita la standul de testare a emisiilor poluante: a fost prezentată procedura standardizată urmată pentru determinarea și certificarea nivelului de emisii poluante ale autovehiculelor.

Ultima zi a evenimentului a fost dedicată recunoașterii implicării







studenților, experților RAR și cadrelor didactice din ATM FI, găzduind festivitatea de înmânare a diplomelor de participare la sediul Academiei Tehnice Militare "Ferdinand I".
Școala de Vară UNIvIA 2026 reprezintă o etapă importantă în pregătirea profesională a studenților, consolidând legătura dintre mediul academic, instituțiile de reglementare și industria de automobile civile și militare.

Conf. univ. dr. ing. Daniela VOICU
Academia Tehnică Militară „Ferdinand I" București

Continuare de la pagina 3

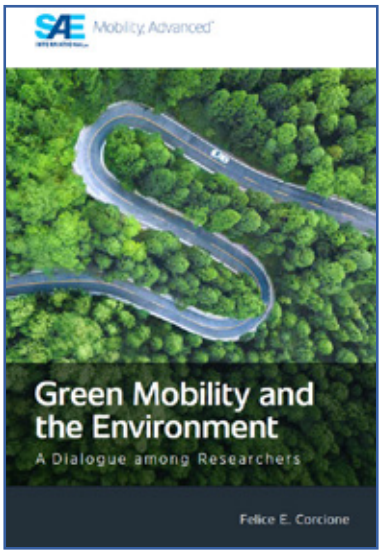
Chiar „inginer senior" fiind, nu ar primi responsabilitatea proiectării unui motor cu adere internă de unul singur! Realitatea este că astfel de proiecte sunt încredințate unor colective complexe ce includ ingineri din generații diferite și cu specializări diferite! Aici, a se avea în vedere că pun problema procesului de proiectare și nu a instrumentelor folosite în cadrul procesului de proiectare.
Un alt comentariu ar fi că pentru un colectiv de o sută de studenți cadrul didactic ar trebui să formuleze o sută de teme de proiect diferite, dar având ca obiect principal același produs – spre exemplu un motor cu ardere internă! Si asta în fiecare an! An după an!
Fără a mai dezvolta, este evidentă o ruptură majoră între obiectivul activității didactice – asimilarea și dezvoltarea deprinderii de a elabora proiecte profesionale - și specificul evaluării și notării proiectului realizat – cu atât mai mult cu cât acesta a fost întocmit cu sprijinul sau de către AI! Am folosit în discuțiile cu colegii amintiți o similitudine: cum ar trebui să se desfășoare aprecierea rezultatului muncii unui olar căruia i se cere să realizeze un ulcior! Aplicând ceea ce știm, vom acorda o notă ulciorului! La proiectul de motoare vom acorda o notă lucrării prezentate de student! Așadar, vom fi atenți mai ales la produs (așa cum am menționat deja - realizat în cea mai mare parte „acasă" – eventual cu ajutorul sau de către AI) și nu la procesul de realizare a produsului – adică la procesul de proiectare – de fapt obiectivul evident al activității didactice specifice! Dacă în concepția de formare a inginerilor de autovehicule vom schimba modul în care abordăm componenta didactică destinată obținerii/însușirii deprinderilor de proiectare (elaborarea de proiecte profesionale) mutând evaluarea și notarea de pe rezultat (proiect) pe proces - adică pe însușirea modului în care se proiectează un motor cu ardere internă, un reductor, o casetă de direcție etc., atunci am aduce AI la locul ei – instrument/asistent/ajutor al inginerului în procesul de creație! Instrument și nu substituent! Atunci am privi (și aprecia) munca olarului și nu la ulcior, indiferent cât de bine ar arăta!
Ca urmare, pentru acest tip de activități didactice consider că ar fi oportună o schimbare fundamentală în ideea evaluării și notării procesului de elaborare a proiectului și nu a proiectului final! Să evaluăm și să notăm procesul de realizare a ulciorului și nu ulciorul! Asta ar presupune schimbări semnificative pentru toți cei implicați – cadre didactice, administrație, studenți/absolvenți! Înclin să cred că de voie, de nevoie, schimbările vor veni!

Aspectele abordate în acest editorial sunt deosebit de complexe si implică elemente diferite – de la etica profesională, corectitudine, egalitate de șanse, responsabilitate individuală și instituțională la viziuni sistemice concentrate pe procese.
Consider că este necesară inițierea în cadrul SIAR a unei dezbateri pe tema prezenței AI în formarea inginerilor de automobile (și nu numai)! SIAR poate asigura spațiul unor astfel de dezbateri, iar implicarea membrilor SIAR (seniori, juniori și titulari) este imperativă! Dezbaterile online ar putea asigura un acces larg și un schimb important de opinii și experiențe! Iar obținerea unei viziuni coerente a școlii românești de automobile asupra rolului AI cel puțin în domeniul ingineriei autovehiculelor, transporturilor și securității rutiere este necesară.
Deviza SIAR este „Cunoaștere și dezvoltare prin cooperare!"
Împreună putem croi un viitor mai bun!

Prof. univ. emerit dr. ing. Minu MITREA
Secretar General SIAR

[1] https://www.europarl.europa.eu/topics/ro/article/20200827STO85804/ce-este-inteligenta-artificiala-si-cum-este-utilizata
[2] https://www.gatesnotes.com/a-turbulent-ai-era-and-critical-choices-to-make
[3] https://www.youtube.com/watch?app=desktop&v=pJ-TBE7HaiA&ra=m
[4] ARACIS – Standarde specifice programe de studii universitare de licență – aprilie 2025, Anexa 2 Domeniul fundamental 2 Stiinte ingineresti 2025

GREEN MOBILITY AND THE ENVIRONMENT: A DIALOGUE AMONG RESEARCHERS



Autor (Author): FELICE ESPOSITO CORCIONE
Editura (Published by): SAE International
Anul apariției (Published): 2024
ISBN: 978-1-4686-0801-4

Din introducerea autorului / Author's foreword – Professor Felice E. CORCIONE:

„Since 1974, I have always been involved in the fluid dynamics and combustion of endothermic engines, my aim being the minimization of harmful exhaust emissions by way of hydrogen and green hydrogen fuel cells as an alternative to fossil fuels. After carefully analyzing the current environmental situation and the repeated (albeit varying) proposals of the European Union from 2020 to 2050 regarding sustainable mobility, I invited colleagues from the National Research Council (CNR) Motor Institute, experts from the CNR Institute of Science and Technology for Sustainable Energy and Mobility from the University of Naples, and members of the corporate world to evaluate and compare the positive climate impacts of internal combustion engines vehicles equipped with new "green" technologies. Mariano Migliaccio, professor of internal combustion engines at the University of Naples (retired) welcomed the invitation with enthusiasm along with Giuseppe Police, former director of Istituto Motori (retired). The meeting was held on Saturday, April 16, 2022, in Avellino, in Prata di Principato Ultra, at Via Vicinale Maurisi, home of my agricultural company—Vigna Maurisi—founded in 2011 to produce Greco di Tufo DOCG and Irpinia Aglianico POD grapes. They are grown in the biodynamic method, with utmost respect to environmental balance. The chosen place is not random. The vineyard is near Pianodardine of Pratola Serra, home of Stellantis Hordain, recently formed by the merger between Fiat Chrysler Automobiles (FCA) and the French PSA Group. Stellantis Hordain is focusing its production on eco-friendly electric and hydrogen vehicles. Upon reaching the farm, the full rebirth of flora and fauna is felt. At this time of year, the vines are in full bloom, the air is warm, the sky is clear of clouds, and the lizards run quickly to conquer a place in the sun. You can even see traces of the herds of wild boar looking for roots to feed on. Everything around favors scholarly dialogue among old research friends. Under the porch of the farmhouse, we enjoy glasses of Greco di Tufo and a good local cheese, during which I begin our noble conversation: our reason for being here.

Starting with examination of the European perspective,I focus the attention on the following topics:

- *Environmental degradation*
- *Treatment of municipal solid waste*
- *Proposals from the European Union*
- *Biofuels*
- *Synthetic fuels and e-fuels*
- *Hydrogen*

The objective of this book, the search for sustainable scientific citizenship, is the result of our dialogue. The aim is to arouse the curiosity of "citizen readers" regarding current and broad environmental problems and the theoretical and practical aspects of "green mobility." This is a contribution toward a future world of zero-emission mobility."

Capitolele lucrării/ Contents of the book:

Environmental Degradation: *Introduction; Causes of Environmental Degradation; Treatment of Municipal Solid Waste; Landfills; Waste-to-Energy Plants; Agriculture; Transport; Cost Analysis Between Diesel and Electric Cars*

European Union Proposals: *European Union Proposals: Fit for 55; New Proposals and Actions from Europe; Euro 7 Regulation*

The Rebirth of the Planet in the Name of Renewable Energy: *Introduction; Solutions and Remedies; Biofuels; Synthetic Fuels and "E-Fuels"; Circular Economy*

Hydrogen as an Energy Carrier of the Future: *Hydrogen; Different Types of Hydrogen; Hydrogen from Ammonia; Ammonia Engine; The Announcement of Toyota; Is it the Ammonia Era? Energy Revolution; The Cost of Solar; Progress of Nuclear Fusion; New Generation: Waste to Energy Plants; Anaerobic Digestion of the Wet Fraction of Waste; Storage and Transport of Hydrogen; Electrification of Mobility; Hydrogen Technology: Current Trends and Controversies; Low Emission Cars*

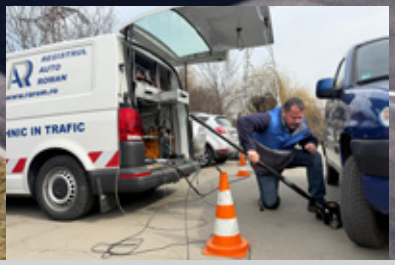
Mega-Trends in Technology: *Epilogue; Conferences and Articles by the Author and Colleagues; Appendix A: Catania 2003: Electric-Fuel Cell Vehicles for Sustainable Mobility; Appendix B: Bressanone 2005: Exhibition and Test of Electric Vehicles; Appendix C: International Journal of Environmental Research and Public Health; Appendix D: Maurisi Vineyard Biodynamic Method; Appendix E: The Internal Combustion Engine; Index; About the Author*

REGISTRUL AUTO ROMÂN





















Programări
la numărul
021/9672
și pe
www.rarom.ro

www.autotestmagazin.ro
www.facebook.com/RegistrulAuto
www.facebook.com/autotestmagazin